Voltage Sensitivity and Gating Charge in *Shaker* and *Shab* Family Potassium Channels

Leon D. Islas and Fred J. Sigworth

From the Department of Cellular and Molecular Physiology, Yale University School of Medicine, New Haven, Connecticut 06520

abstract The members of the voltage-dependent potassium channel family subserve a variety of functions and are expected to have voltage sensors with different sensitivities. The *Shaker* channel of *Drosophila*, which underlies a transient potassium current, has a high voltage sensitivity that is conferred by a large gating charge movement, ~13 elementary charges. A *Shaker* subunit's primary voltage-sensing (S4) region has seven positively charged residues. The *Shab* channel and its homologue Kv2.1 both carry a delayed-rectifier current, and their subunits have only five positively charged residues in S4; they would be expected to have smaller gating-charge movements and voltage sensitivities. We have characterized the gating currents and single-channel behavior of *Shab* channels and have estimated the charge movement in *Shaker*, *Shab*, and their rat homologues Kv1.1 and Kv2.1 by measuring the voltage dependence of open probability at very negative voltages and comparing this with the charge–voltage relationships. We find that *Shab* has a relatively small gating charge, ~7.5 e_o. Surprisingly, the corresponding mammalian delayed rectifier Kv2.1, which has the same complement of charged residues in the S2, S3, and S4 segments, has a gating charge of 12.5 e_o, essentially equal to that of *Shaker* and Kv1.1. Evidence for very strong coupling between charge movement and channel opening is seen in two channel types, with the probability of voltage-independent channel openings measured to be below 10^{-9} in *Shaker* and below 4×10^{-8} in Kv2.1.

key words: ion channels • patch-clamp • gating current • kinetics

INTRODUCTION

Voltage-gated ion channels are remarkably sensitive to membrane potential changes. Large charge movements in the channel protein couple changes in membrane potential to the channel opening process. In the skeletal muscle sodium channel and the *Shaker* potassium channel, the size of this "gating charge" movement is seen to be equivalent to the displacement of 12–14 elementary charges entirely across the membrane (Hirschberg et al., 1995; Schoppa et al., 1992; Aggarwal and MacKinnon, 1996; Noceti et al., 1996). The large charge movement makes sense for the sodium channel, where the resulting high sensitivity helps to establish a firing threshold for excitable cells. For transient potassium channels such as *Shaker*, the high sensitivity is important to allow channel activation during threshold depolarization, enabling these channels to control repetitive firing rates in neurons (Neher, 1971; Connor and Stevens, 1971a,b). On the other hand, high voltage sensitivity in delayed-rectifier potassium channels is arguably less important: these channels need only be activated by the large excursions of action potentials, and indeed the presence of large charge movements can be detrimental. As pointed out by Hodgkin (1975), gating charge movements serve as a capacitive "load" on the action potential, increasing metabolic requirements and decreasing the velocity of action potential propagation in excitable cells.

The various voltage-gated potassium channels contain four α subunits; many of these subunits show differences in their S4 regions that are suggestive of differing amounts of gating charge. The S4 region is thought to be the primary voltage-sensing region (Stühmer et al., 1989; Aggarwal and MacKinnon, 1996; Seoh et al., 1996); in the *Shaker* family it has seven positively charged residues and in the other potassium channel families it has between four and six. Some mutations in *Shaker* that reduce the number of basic residues reduce the apparent voltage sensitivity, but other mutations leave the voltage sensitivity apparently unchanged (Smith-Maxwell et al., 1998). It should be pointed out that in members of *Shaker* and other related families, the acidic residues in S2 and S3 are conserved; one of these, the second glutamate in S2, has also been implicated in the voltage-sensing function (Seoh et al., 1996).

Because of uncertainties in past measurements of charge movement based on voltage sensitivity, and to complement the studies in which the magnitude of gating charge has been changed through mutations, we report here measurements of the gating charge in four "native" voltage-gated potassium channel types using improved methods.

Gating charge movement is most directly measured by integrating the gating currents that are recorded

Address correspondence to Dr. Fred J. Sigworth, Department of Cellular and Molecular Physiology, Yale University School of Medicine, 333 Cedar Street, New Haven, CT 06520. Fax: 203-785-4951; E-mail: fred.sigworth@yale.edu

J. Gen. Physiol. © The Rockefeller University Press • 0022-1295/99/11/723/19 $5.00
Volume 114 November 1999 723–741
Released online 25 October 1999
http://www.jgp.org

from membranes having a high density of channels, under conditions in which no ionic current flows through the channels. To then evaluate the charge movement in a single channel, the number of channels contributing to the gating current must be estimated; this has been done for *Shaker* channels using either fluctuation analysis (Schoppa et al., 1992; Seoh et al., 1996; Noceti et al., 1996) or radioligand binding (Aggarwal and MacKinnon, 1996). The results of the two methods agree well, yielding values of the single-channel charge of 12–14 e_o. An alternative approach is called the "limiting-slope" method, and is analogous to the determination of the Hill coefficient of a binding reaction. It involves measuring the dependence of the channel open probability, *P*, on membrane potential V. Given a channel that opens with depolarization and has a single open state, then asymptotically, as $V \rightarrow -\infty$ (and $P \rightarrow 0$), the apparent charge,

$$q_s(\mathrm{V}) = kT\frac{d\ln P(V)}{dV}, \qquad (1)$$

approaches the total charge movement q_T (Almers, 1978). The limiting-slope method has been applied to *Shaker* and some mutants (Noceti et al., 1996; Seoh et al., 1996) and its results are in good agreement with the direct charge measurements outlined above.

The limiting-slope method has the advantage that it measures charge that is actually involved in opening the channel. Its asymptotic nature, on the other hand, poses a problem: how can one be sure that q_s is evaluated at sufficiently negative *V*? Two recent advances now allow this problem to be addressed in a rigorous fashion. The first is the development by Hirschberg et al. (1995) of a method for measuring very small *P* values at the very negative membrane potentials where one hopes that the asymptotic limit is reached. The method involves measuring single-channel events in membrane patches having large numbers of channels *N*. For channels having brief open times, the aggregate open probability *NP* can be measured in such patches down to values of 10^{-4} or less; with *N* on the order of 10^3, *P* can be reliably estimated down to values of 10^{-7} or less.

The second advance is the theory of Sigg and Bezanilla (1997), which shows that an ordinary gating current measurement can be used as an independent test of the extrapolation of q_s values to estimate q_T. Let $\hat{Q}(\mathrm{V})$ be the macroscopic gating charge that is obtained by integrating the gating current, normalized such that $\hat{Q}(-\infty) = 0$ and $\hat{Q}(+\infty) = 1$. Then, in the case of a channel that is found in its single open state at large depolarizations, the apparent charge q_s is related to $\hat{Q}$ by:

$$q_s(\mathrm{V}) = q_T[1 - \hat{Q}(\mathrm{V})]. \qquad (2)$$

Thus, given experimentally determined values of q_s and $\hat{Q}$, a one-parameter curve fit can be used to estimate the value of q_T.

In this paper, we incorporate these advances to the limiting-slope method and apply it to the determination of charge movements in homomeric channels encoded by the *Drosophila* potassium channel genes *Shaker* and *Shab*, and from the rat homologues Kv1.1 and Kv2.1. A comparison of these channel types is interesting in view of their differing amino acid sequences (Fig. 1). *Shaker* and Kv1.1 both have seven basic residues in the S4 region, while *Shab* and Kv2.1 have five.

MATERIALS AND METHODS

Channel Expression in Oocytes

Shaker H4 with N-type inactivation removed and the W434F mutant were subcloned into the vector pGEM, linearized with Not I and transcribed with T7 RNA polymerase. The final cRNA concentration was 1 μg/μl. Kv1.1 was subcloned into pGEMHE, linearized with PstI and transcribed using T7 polymerase. *Shab* was subcloned in a modified version of Bluescript for oocyte experiments. Linearization of cDNA was carried out with NotI and transcription with T3 polymerase.

The rat clone Kv2.1-Δ7 (DRK1-Δ7), derived from DRK1 (Frech et al., 1989) was provided by Drs. R. MacKinnon (The Rockefeller University, New York, NY) and S. Aggarwal (Harvard Medical School, Cambridge, MA). This construct has seven point mutations in the putative pore mouth that permit very high affinity binding ($K_d \approx 15$ pM) of the channel blocker Agitoxin-1 (Gross et al., 1994). Kv2.1-Δ7 in Bluescript was linearized with NotI, transcribed with T7 RNA polymerase and resuspended in water to a final concentration of 0.3–0.5 μg/μl.

Xenopus laevis oocytes were harvested under anesthesia and defolliculated by incubation in Ca^{+2}-free OR2 solution supplemented with 2 mg/ml collagenase 1A for 1 h. Oocytes were incubated at 20°C in a solution containing (mM): 96 NaCl, 2 KCl, 1.8 $CaCl_2$, 1 $MgCl_2$, 5 HEPES, and injected 1 or 2 d after harvesting with 50 nl of cRNA solution with a Nanostepper (Drummond Scientific Co.) using pipettes of 20-μm opening diameter. Oocytes were used for experiments 1–7 d after injection.

In some cases, oocytes expressing Kv2.1-Δ7 were incubated in the presence of Agitoxin-1 at a concentration of 1–3 μM for the period of channel expression. This resulted in an increase in expression of two- to threefold.

Expression of Channels in Sf9 Cells

The *Shab* channel was expressed in Sf9 cells for the recording of gating currents in whole cells. The Bac-to-Bac™ recombinant baculovirus system (GIBCO BRL) was used. After transfer of the *Shab* gene to a bacmid vector, Sf9 cells at 70% confluence were transfected with lipofectin in Sf900 medium (GIBCO BRL). The culture medium containing the *Shab* baculovirus was collected after 48 h of culture and stored at 4°C. After infection, expression of channels in cells was assessed by electrophysiological recording. Sf9 cells were maintained in an incubator at 26°C in 1% CO_2.

Patch Recording

Patch-clamp recordings were obtained using standard techniques. All recordings reported here were made in the cell-attached configuration, for maximum patch stability. Oocytes were bathed in a depolarizing solution that effectively zeroed the

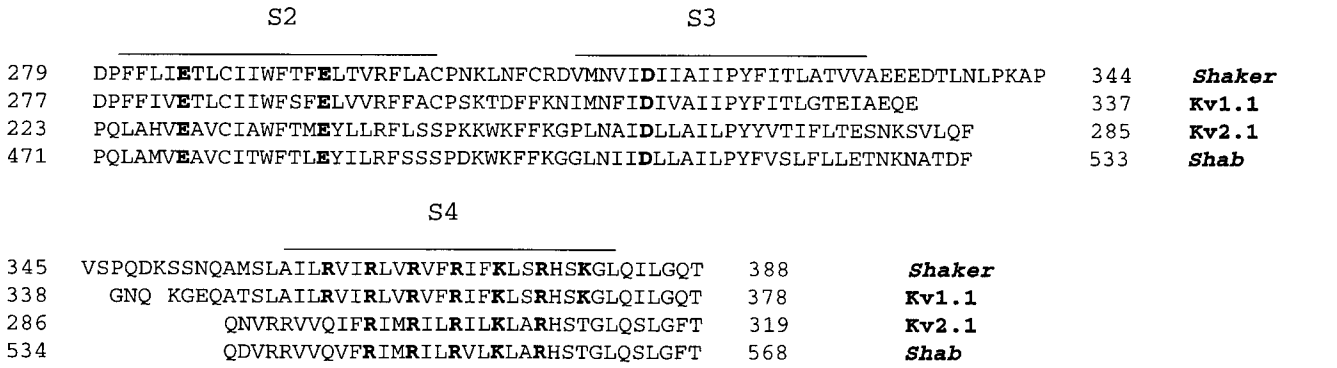

Figure 1. Sequence alignment of the S2–S4 regions of the four voltage-gated potassium channels in this study. The proposed membrane spanning regions are indicated by lines. Bold letters indicate conserved charged residues. Numbers at the beginning and end of each segment refer to amino acid numbering. *Shaker* numbering corresponds to the *Shaker* B1 splice variant (Schwarz et al., 1988). Sequences are taken from Chandy and Gutman (1995).

membrane potential as checked with a two-microelectrode voltage clamp. The bath solution contained (mM): 120 K-aspartate, 20 KCl, 1.8 $CaCl_2$, 10 HEPES, adjusted to pH 7.4. Unless otherwise stated in the figure legends, pipettes were filled with a solution of the following composition (mM): 40 K-aspartate, 20 KCl, 1.8 $CaCl_2$, 60 *N*-methyl-d-glucamine (NMDG)[1]-aspartate, 10 HEPES, pH 7.4. Gating currents of Kv2.1-Δ7 were recorded using a similar solution that contained 120 mM NMDG-aspartate and no K^+, and included 1 μM Agitoxin-1. The same solution was used for *Shaker* gating currents without the Agitoxin-1. For gating currents, 20 sweeps were averaged at every voltage. A P/5 subtraction protocol was used to subtract linear capacity and leak currents, using a leak-holding potential of −120 mV.

Pipettes were pulled from soft borosilicate glass capillaries (Kimax-51) and had resistance in the range 1.5–3 MΩ. Currents were recorded with an EPC-9 amplifier running the Pulse software (HEKA Elektronik) on a Macintosh computer. In macroscopic current recordings, the linear current components were subtracted by the use of a P/5 protocol and were filtered at 2.5 kHz (−3 dB) with a Bessel filter and sampled at 15 kHz. Single-channel recordings were obtained in the same patches as macroscopic currents, with the same filter cut-off frequency and a sample frequency of 10 kHz. Null-trace averages were used to subtract the linear capacitive and leak currents. All recordings were obtained at room temperature (22°C).

Whole-cell gating currents in Sf9 cells were recorded using the following solutions (mM): Pipette: 150 NMDG-HCl, 10 MOPS, 5 EGTA, 1 $MgCl_2$, pH 7.2; Bath: 150 NMDG-HCl, 10 MOPS, 10 $CaCl_2$, 1 $MgCl_2$, pH 6.7. Recording electrodes had a resistance of 0.5–1 MΩ and were coated with Sylgard® to reduce capacitance. No series resistance compensation was used. The capacitance of the Sf9 cells used for gating current recordings ranged from 20 to 42 pF. The settling time of capacity transients was ∼100 μs. The subtraction protocol was similar to that used for Kv2.1.

Data Analysis

For macroscopic currents, the voltage dependence of the open probability was estimated from tail current measurements; the size of the tail current is proportional to the channel open probability at the end of the preceding depolarization. We averaged the first millisecond of tail current at −100 mV in the case of Kv2.1 channels. For *Shaker* and *Shab*, the first 300 μs of tail currents at −90 mV were averaged and for Kv1.1, 400 μs was averaged. The values obtained were in very close agreement to the more traditional method of measuring *P* from the steady state currents and normalizing by the instantaneous current–voltage curve. Contamination of the ionic tail currents by gating currents was taken to be negligible because OFF gating current amplitudes were <0.5% of the maximal tail current amplitude.

Estimation of the number of channels in a patch of membrane was done by nonstationary noise analysis (Sigworth, 1980; Heinemann and Conti, 1992). The mean and variance were calculated from 50–60 current traces elicited by depolarizing steps to the indicated membrane potential filtered at 5 kHz. Pulses were delivered at 0.5-s intervals. The variance estimation made use of groups of four sweeps, to reduce the influence of drifting baselines and channel rundown. The data were displayed in the form of mean-variance relationships and fitted to the equation:

$$\sigma^2 = iI - \frac{I^2}{N},$$

where σ^2 is the variance, I is the mean current, i is the single channel current, and n is the number of channels. The maximal open probability was then obtained as $P_{max} = I_{max}/Ni$.

The analysis of the single channel traces to obtain the time-dependent *NP* values was carried out as follows. The current traces were leak subtracted using a template of averaged null sweeps (sweeps that contain no channel openings), digitally filtered with a Gaussian filter to 1.5 kHz and analyzed with the 50% threshold crossing method (Colquhoun and Sigworth, 1995) with multiple thresholds to allow detection of overlapping channel currents. This produced an idealized record of open and closed events. The idealizations of 100–1,000 sweeps were then averaged, with null traces included. The steady state average value, typically computed from the last 150 ms of the averaged idealization, was taken as the final value for *NP*. Open and closed dwell time histograms were obtained using a single threshold from sweeps with no overlapping openings and constructed according to the log-binning technique (Sigworth and Sine, 1987) and probability density functions were fitted by the method of maximum likelihood.

The apparent charge q_s was estimated from experimental data by discretizing Eq. 1 in the following way. Given open probabilities P_1 and P_2 obtained at adjacent voltages V_1 and V_2, and letting $V' = (V_1 + V_2)/2$, we computed q_s as:

$$q_s(V') = kT\frac{\ln P_1 - \ln P_2}{V_1 - V_2}.$$

[1]*Abbreviation used in this paper:* NMDG, *N*-methyl-d-glucamine.

The equilibrium voltage dependence of state occupancies was computed according to Eq. 3:

$$P_n(V) = \frac{\prod_{j=1}^{n} K_j(V)}{\sum_{i=1}^{M} \prod_{j=1}^{n} K_j(V)}, \quad (3)$$

where P_n is the probability of occupancy of state n, K_j is the equilibrium constant for transition from state $j-1$ to state j, and the M states are linearly connected.

Statistical quantities are given as mean ± SEM

RESULTS

Channel Activation Properties

To extend the previous studies of *Shab* channel currents (Tsunoda and Salkoff, 1995), we first compare *Shab* channel properties with those of the other channel types. For this study, we have used a *Shaker* construct having a deletion at the NH_2 terminus to remove fast inactivation, to simplify the determination of steady state open probability. For Kv2.1, we have used a mutant, DRK1-Δ7, that was engineered to bind the pore blocker Agitoxin-1 with high affinity (Aggarwal and MacKinnon, 1996; Gross et al., 1994), making possible the measurement of gating currents. Macroscopic currents were obtained in cell-attached patch recordings from mRNA-injected oocytes or in whole-cell recordings from recombinant baculovirus-infected Sf9 cells in the case of *Shab* channels. Representative current traces are shown in Fig. 2 A. The channel open probabilities *P* for each channel type approach limiting values between 0.7 and 0.9 for large depolarizations. The voltage-dependence of *P* for *Shaker* and Kv1.1 (Fig. 2 B) can be described well by the fourth power of a Boltzmann function, as would be predicted by a simple model incorporating four independently acting voltage sensors (Zagotta et al., 1994). The gating charges estimated from these fits are 11.5 and 7.7 e_o for *Shaker* and Kv1.1, respectively; it should be emphasized, however, that such gating-charge estimates are strongly dependent on the particular model used. The corresponding fit to the *P–V* relationship for *Shab* channels yields an apparent charge of 6.3 e_o, while for Kv2.1 it yields 10.1 e_o (Fig. 2 C).

Activation time constants τ were estimated from exponential fits to the second half of the activation time course of macroscopic currents (Schoppa and Sigworth, 1998a). From these fits an estimate of the delay in activation δ was also obtained. *Shaker* channels show a small activation time constant that is rather weakly voltage dependent with an effective charge of 0.51 e_o; the delay is roughly equal to the time constant and has similar voltage dependence (Fig. 2, D and E) over the positive voltage range. The kinetic features of Kv1.1 channels are nearly identical to those of *Shaker*, having almost identical activation time constants and delay values, with the main difference being a slightly steeper activation curve.

Like *Shaker*, *Shab* channels activate and deactivate quickly, with time constants similar to those of *Shaker*. *Shab* channels activate, however, with a smaller delay that is more steeply voltage dependent (Fig. 2 E); this means that at positive voltages these channels show less sigmoidicity in their activation time course than *Shaker* (Zagotta et al., 1994; Smith-Maxwell et al., 1998). This behavior can be explained if the rate-limiting step for activation (which determines τ; Schoppa and Sigworth, 1998a) is less voltage dependent than other steps that determine the delay. The same general phenomenon is seen in Kv2.1, although here the much slower activation is reflected by τ and δ having values that are larger by an order of magnitude.

Gating Currents

The time course of charge movement of *Shaker*, Kv2.1, and *Shab* channels was directly measured in the form of gating currents. *Shaker* gating currents were obtained from cell-attached patches in oocytes expressing the nonconducting mutant W434F (Perozo et al., 1993) using the same solutions as those used to record macroscopic ionic currents. The voltage dependence of the charge obtained from integration of ON gating currents is similar to that previously reported, as is the decay time constant of ON currents (Fig. 3, B and C).

Kv2.1 gating currents were also measured in cell-attached patches in oocytes, using Agitoxin-1 to block the ionic currents. The general characteristics are similar to those previously reported (Taglialatela and Stefani, 1993) from the cut-open oocyte recording technique. ON gating current decays are approximately five times slower than *Shaker*'s (at 0 mV), but show a steeper voltage dependence of the time constant. Taglialatela and Stefani (1993) observed gating current decay time constants that were very close to the ionic current time constants; however, under our recording conditions and with the mutant channel that we are using, the gating current time constants are severalfold shorter than the ionic current time constants. Thus, we observe a gating current time constant that is similar to the delay of ionic currents but is shorter than the activation time constant. This can be explained if the gating current comes predominantly from early voltage-dependent transitions that give rise to the ionic current delay, and the rate-limiting step comes later in the activation process.

The Kv2.1 charge movement curve lies to the left of the $P(V)$ curve in the voltage axis, as is expected for a channel that has multiple closed states before the open state. The voltage dependence of charge can be fitted to a Boltzmann function with a charge of 2 e_o (Fig. 3 B).

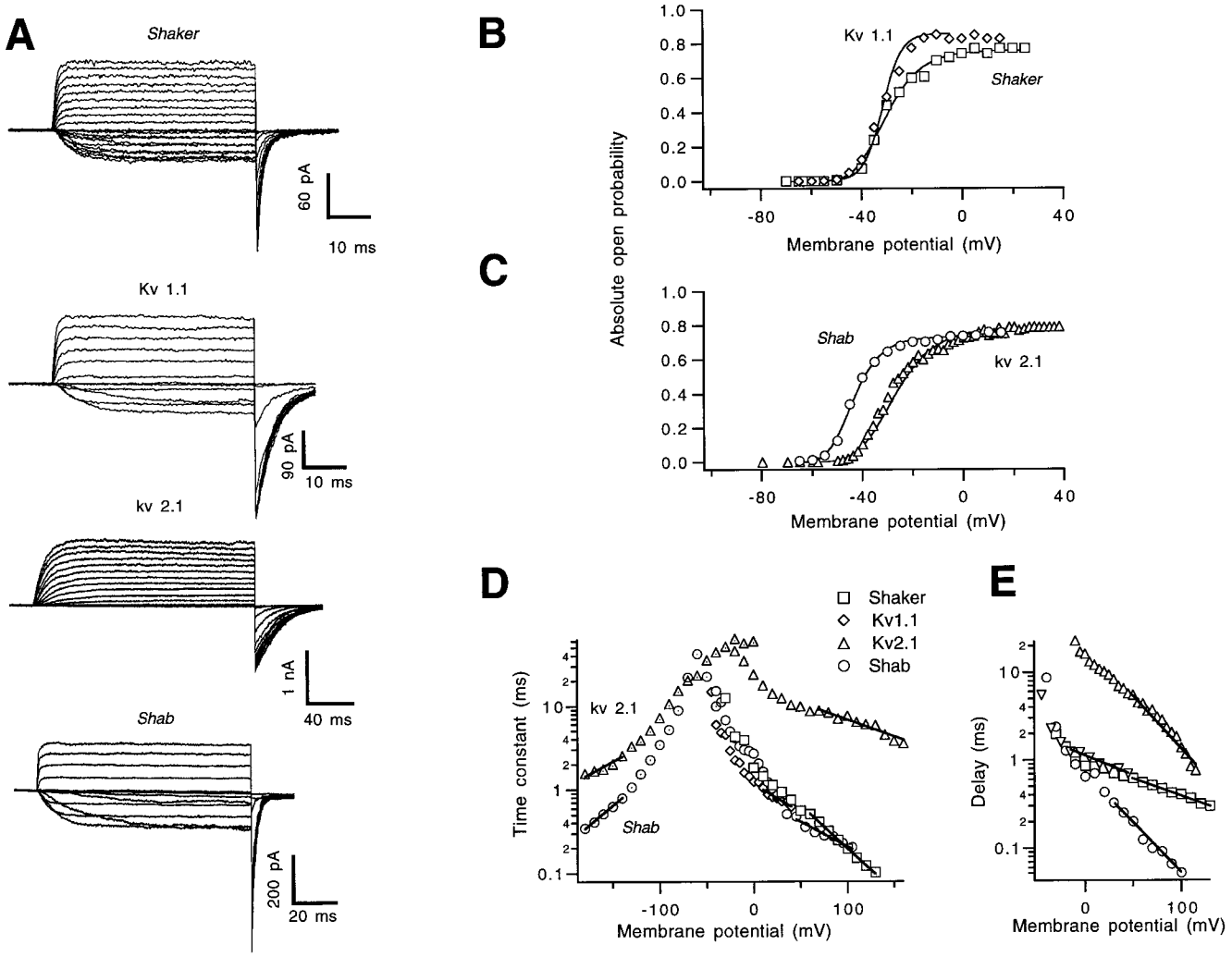

Figure 2. Macroscopic activation properties of *Shaker*-related potassium channels. (A) Current traces in cell-attached patches in response to depolarizing voltage steps. The holding potential is −80 mV in each case except −90 for *Shab*. The voltage range for the depolarizations is as follows: *Shaker*: −58 to 26 mV in 4-mV steps; Kv1.1: −65 to 55 mV in 10-mV steps; Kv2.1: −50 to 40 mV in 5-mV steps; *Shab*: −70 to 50 mV in 10-mV steps. In each case, the standard pipette solution was used, which contained 60 mM K^+. Recordings are from oocyte patches, except for *Shab*, which is from an Sf9 cell patch. Increased noise in the largest Kv2.1 currents presumably comes from internal Mg^{2+} block of these channels (Lopatin and Nichols, 1994). (B) Voltage dependence of activation obtained from tail currents. The tail current amplitude was taken to be proportional to the open probability at the end of the voltage pulse. Values were normalized to the maximum P obtained from nonstationary noise analysis at 60–70 mV. The P_{max} values are 0.79 for *Shaker* and 0.82 for Kv1.1. The $P(V)$ relationship was fitted to the fourth power Boltzmann function:

$$P(V) = P_{max}\left[\frac{1}{1 + e^{-q/kT(V - V_0)}}\right]^4,$$

where V is the voltage in millivolts, q is the charge per subunit in (e_o), V_0 is the half-activation voltage, and kT has its usual meaning. The fitted values are: *Shaker*, $V_o = -27.5$ mV and $q = 2.88$ e_o. Kv1.1, $V_o = -33.4$ mV and $q = 1.92$ e_o. (C) Voltage dependence of activation for Kv2.1 and *Shab* channels. P_{max} values are: Kv2.1, 0.69; *Shab*, 0.76. The fitted parameters are: Kv2.1, $V_o = -22.4$ mV and $q = 2.53$ e_o. *Shab*, $V_o = -44.9$ mV and $q = 1.56$ e_o. (D) Voltage dependence of activation and deactivation time constants τ, and (E) delay of activation δ. The values at voltages above 50 mV, or 0 mV in the case of Kv1.1, were fitted to the functions: $\tau(V) = \tau(0)\exp(Vq_\tau/kT)$ and $\delta(V) = \delta(0)\exp(Vq_\delta/kT)$, where q_τ and q_δ are partial charges associated with the time constant and the delay, respectively. Fitted values are as follows: Kv2.1 (△): $q_\tau = 0.24$ e_o, $q_\delta = 0.62$ e_o; *Shab* (○): $q_\tau = 0.30$ e_o, $q_\delta = 0.7$ e_o; *Shaker* (□): $q_\tau = 0.51$ e_o, $q_\delta = 0.22$ e_o; and Kv1.1 (◇): $q_\tau = 0.37$ e_o, $q_\delta = 0.28$ e_o. The symbols with a dot indicate deactivation time constants derived from exponential fits of tail currents at the indicated potentials for Kv2.1 and *Shab*. The effective charge q_δ in the most negative potential region is Kv2.1 = −0.32 e_o; *Shab* = −0.43 e_o.

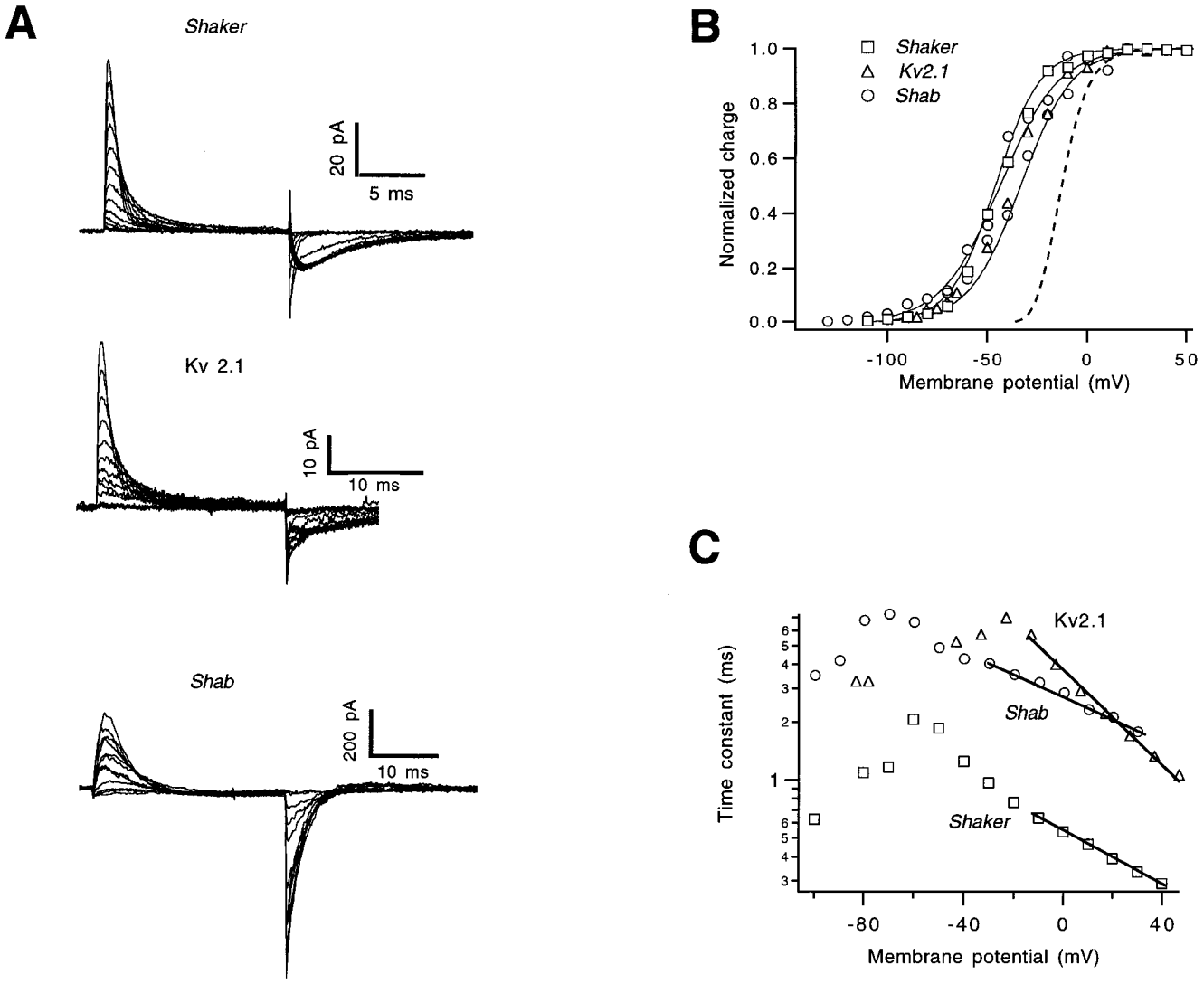

Figure 3. Gating currents from *Shaker*, Kv2.1, and *Shab* channels. Gating currents were recorded in the cell-attached configuration in the case of *Shaker* and Kv2.1, and in whole-cell for *Shab*. (A) Representative traces of gating currents recorded from a holding potential of −100 mV (Kv2.1) or −90 mV (*Shaker* and *Shab*) in 10-mV increments. Test pulses for *Shaker* are from −110 to 10 mV; for Kv2.1 from −85 to 45 mV; and for *Shab* from −140 to 20 mV. (B) Voltage dependence of the normalized charge movement obtained from numerical integration of the ON gating currents. The dashed curve represents the voltage dependence of activation of Kv2.1 macroscopic currents and is shown for comparison. Continuous curves are fits to a Boltzmann function with the parameter values: *Shaker* $q_s = 2.24\ e_o$, $V_o = -45.9$ mV; Kv2.1 $q_s = 1.98\ e_o$, $V_o = -34.9$ mV; *Shab* $q_s = 1.2\ e_o$, $V_o = -43.6$ mV. (C) The voltage dependence of the time constant derived from a single exponential fit to the decaying phase of ON gating currents. Symbols are as in B. The data in the depolarized voltage range were fitted to exponential function of voltage to yield partial charge values $q_{on} = 0.39$, 0.69, and 0.33 e_o for *Shaker*, Kv2.1, and *Shab*, respectively.

Shab gating currents were recorded in the whole-cell configuration from baculovirus-infected Sf9 insect cells, with ionic currents eliminated through the use of impermeant *N*-methyl glucamine (NMG) cations. Fig. 3, B and C, compares the voltage dependence of ON charge and the voltage dependence of the time constant of ON currents in these channels. *Shab* ON gating currents are less voltage dependent than those of *Shaker* or Kv2.1, and their kinetics are intermediate. *Shab* OFF gating currents are, however, very different in having a much faster time course than the others. The slow OFF time course in *Shaker* channels arises from slow initial closing transitions (Zagotta et al., 1994; Schoppa and Sigworth, 1998a); in *Shab*, these transitions presumably proceed much more quickly.

Limiting-Slope Measurements in Shaker Channels

With the high expression obtained with *Shaker* in oocytes, it was possible to record from patches containing hundreds or thousands of channels. The number *N* of channels in a patch was estimated by nonstationary

fluctuation analysis, using depolarizations to +70 mV. Subsequent recordings using small depolarizing pulses allowed *NP* to be estimated from the statistics of single-channel events in the same patch. Recordings from a representative patch containing 2,250 channels are shown in Fig. 4 A. The channel openings observed during the small depolarizations were identified as *Shaker* channels based on their conductance and kinetics.

To obtain the steady state open probability from pulsed data sweeps, we first performed an idealization of the single channel events for each sweep, and then averaged these idealized records. This ensemble average (Fig. 4 B) represents the product *NP* of the open probability and the number of channels that contribute to the record. No inactivation is visible in these time courses, and because of the high external K^+ concentration the degree of slow "C-type" inactivation on these channels is expected to be very small (Lopez-Barneo et al., 1993), reducing *P* by at most 2% at −60 mV (Yang et al., 1996).

At the most negative voltages (−70 to −55 mV), the value of *NP* changed by about a factor of 10 for each

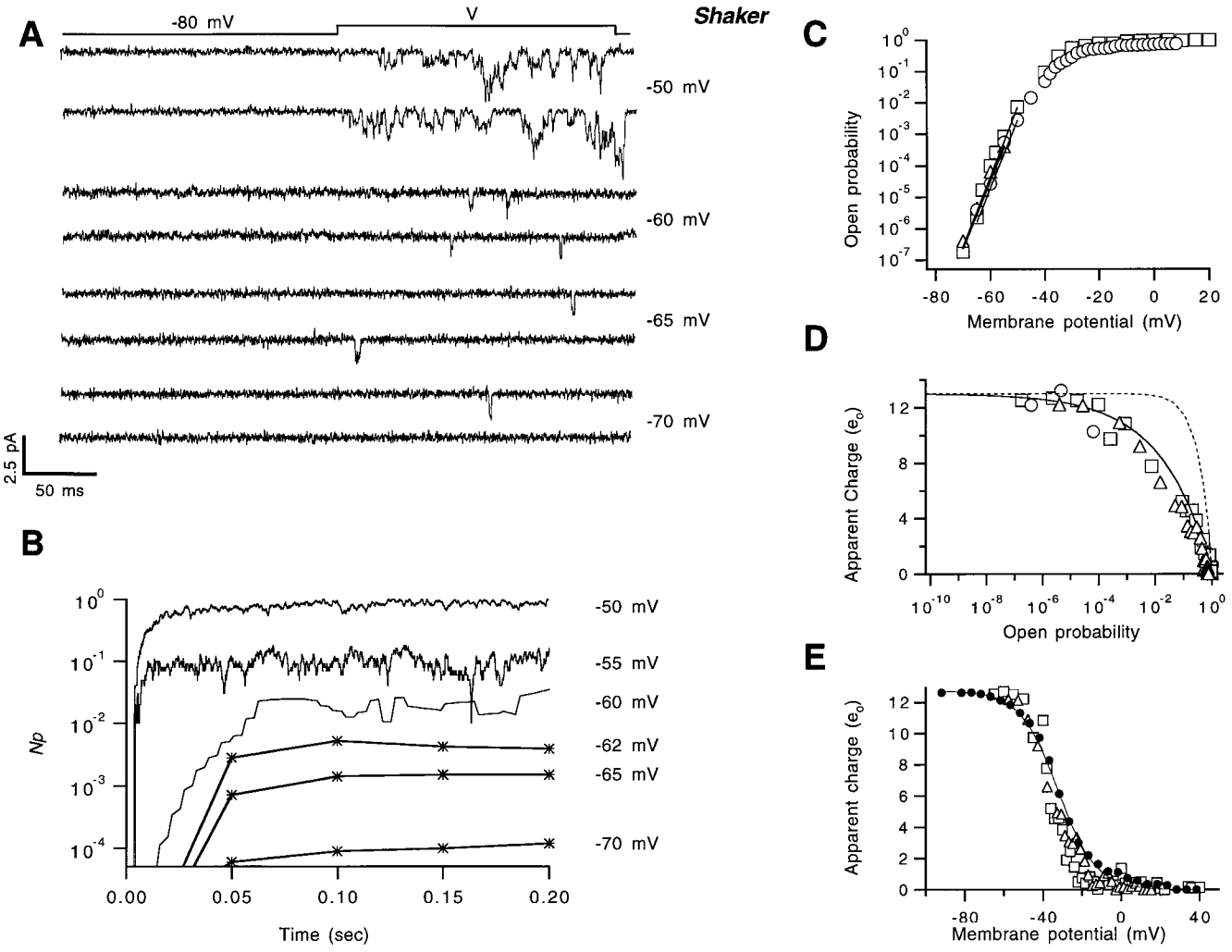

Figure 4. Calculation of the apparent gating charge content from the limiting slope in *Shaker* channels. (A) Representative traces of channel activity in a multichannel patch at the indicated membrane potentials. This patch contained 2,250 channels, as estimated from fluctuation analysis at +70 mV. From a holding potential of −80 mV, pulses of duration 300–400 ms to the indicated potential were applied once per second. (B) The time course of the open probability, reconstructed from sets of 200–300 sweeps at each potential. Note the very steep voltage dependence of steady state open probability (~10-fold/5 mV). During the total of 1,500 sweeps, no channel openings were detected at −80 mV. (C) The $P(V)$ relationships from three experiments are shown with fits (lines) to exponential functions (Eq. 4) over the range $P = 10^{-7}$ to 10^{-3}. The apparent gating charges q_l from these fits are 12.9, 12.4, and 12.8 e_o. (D) The logarithmic slope q_s (Eq. 1) is plotted as a function of *P*. The solid curve is the predicted relationship for a fourth-power Boltzmann function having charge 3.25 e_o per subunit, yielding a total charge 13 e_o. The dashed curve is the relationship for a single Boltzmann function with charge 13 e_o. Different symbols indicate individual patches. (E) Values of q_s plotted against voltage. (●) The macroscopic charge movement $1 - \hat{Q}(V)$ of the W434F mutant recorded under the same conditions in a patch from a different oocyte; it has been scaled to a total charge $q_T = 13$ e_o.

5-mV change in the depolarization. No openings were detected during the total 450 s of recording at the holding potential of −80 mV. At −80 mV, the mean burst duration is expected to be ~1.5 ms so that, were a single opening to occur, it would correspond to $NP \approx 3.3 \times 10^{-6}$. The fact that no events were observed at −80 mV in this patch or in two others having similar numbers of channels implies that at −80 mV P is smaller than $\sim 10^{-9}$.

Fig. 4 C shows the result of combining the single channel data with macroscopic activation measurements and the value of n obtained from nonstationary noise analysis. The smallest open probability measured in these patches was $\sim 10^{-7}$, and the maximum was 0.79. At values of P between 10^{-7} and 10^{-4} the $P(V)$ relation is very nearly exponential and can be well fitted to the relationship

$$P(V) = P(0)\exp(q_l V/kT). \quad (4)$$

The charge estimate q_l from this linear fit to the log-transformed P values represents a local average of q_s as defined in Eq. 1; for these channels it had the value 12.7 ± 0.3 e_o ($n = 3$).

We performed two tests to determine whether these experiments can provide estimates of the apparent charge that approach the true asymptotic value. First, we computed q_s from Eq. 1 at each voltage and compared its behavior with that of two simple models in which P is given by a Boltzmann function or by the fourth power of a Boltzmann function. The comparison is done by plotting the logarithmic slope variable q_s as a function of P, with V being the independent variable (Zagotta et al., 1994; Fig. 4 D). Quite good correspondence is seen with the latter model given a total charge of 13 e_o; were this model correct, our estimated slope q_l would be within 4% of the true limiting slope.

In the second test, $q_s(V)$ is compared with the function, which from Eq. 2 should yield identical values. Fig. 4 E makes this comparison for the case $q_T = 13$ e_o, where it is seen that the voltage dependences are very similar. Most importantly, the charge movement shows very little change below $V = \sim 70$ mV, implying that q_s will remain essentially constant below this membrane potential. On the basis of this fit, we extrapolate the q_s values to obtain an estimate of 13.0 e_o for the total charge q_T.

The Gating Charge of Kv1.1 Is Similar to that of Shaker

Rat Kv1.1 (previously called RCK1) is a potassium channel that does not have fast inactivation. Its general gating characteristics are very similar to those of inactivation-removed *Shaker* and the amino acid sequence in the S4 region is identical (Koren et al., 1990; Fig. 1). Not surprisingly, our limiting-slope estimates of gating charge in Kv1.1 are almost exactly the same as those from *Shaker* channels. Single-channel estimates of *NP* show 10-fold changes for 5-mV changes in membrane potential (Fig. 5, A and B). The apparent gating charge q_l computed for values of P between 10^{-6} and 10^{-4} using Eq. 4, was 11.5 ± 1.3 e_o ($n = 3$). The smallest open probability attained in this measurement was two orders of magnitude higher than in *Shaker*, due to a lower density of channels in patches. Nevertheless, estimates of q_s extrapolate well to a value of $q_T = 13.0$ e_o (Fig. 5 C).

Because of the low channel density, we were unable to record gating currents from patches containing Kv1.1 channels; therefore, we were unable to provide an independent check on the approach to the limiting charge movement. We conclude that q_T is at least 11.5 e_o and is probably near 13 e_o, as is the case with *Shaker*.

Although no inactivation is apparent in the reconstructed time courses of Fig. 5 B, it is conceivable that slow inactivation or rundown could introduce errors into our estimates for P. We therefore compared the N values obtained from noise analysis before and immediately after delivering the 600 depolarizing pulses to −60 and −50 mV for single-channel analysis of one patch; the values of N were 14 and 12, respectively. If the reduction in the number of channels is caused by inactivation, this indicates that there was at most 14% long-term inactivation. In our experiments, this small amount of inactivation at negative voltages would, if anything, have led to an underestimation of the limiting slope.

Limiting-Slope Measurements in Kv2.1 Channels

Previous estimates of the gating charge of the rat Kv2.1 channel (Taglialatela and Stefani, 1993) and the human homologue, hKv2.1 (Benndorf et al., 1994) were in the range 6–7 e_o. These were obtained from model-dependent fitting, a methodology which often underestimates the gating charge. As with *Shaker*, we were able to record from patches containing hundreds of Kv2.1 channels in which we could measure macroscopic currents at depolarizing voltages and resolve single-channel openings at hyperpolarized voltages. Fig. 6 shows recordings from a patch containing ~1,650 Kv2.1 channels.

At the most negative voltages (−45 to −65 mV), the value of *NP* decreased by a factor of ~10 per 5-mV decrease in depolarization (Fig. 6 B). No openings that could be assigned to Kv2.1 channels were detected at the holding potential of −80 mV in two experiments where the total time of recording at −80 mV was 118 and 180 s and the number of channels N was 967 and 1,250, respectively. The channel burst duration, extrapolated to −80 mV, is ~10 ms. Were a single burst of openings to occur in one of these records, this would correspond to the open probability $P \approx 4 \times 10^{-8}$. Therefore, we take the value of P at −80 mV to be less than $\sim 4 \times 10^{-8}$.

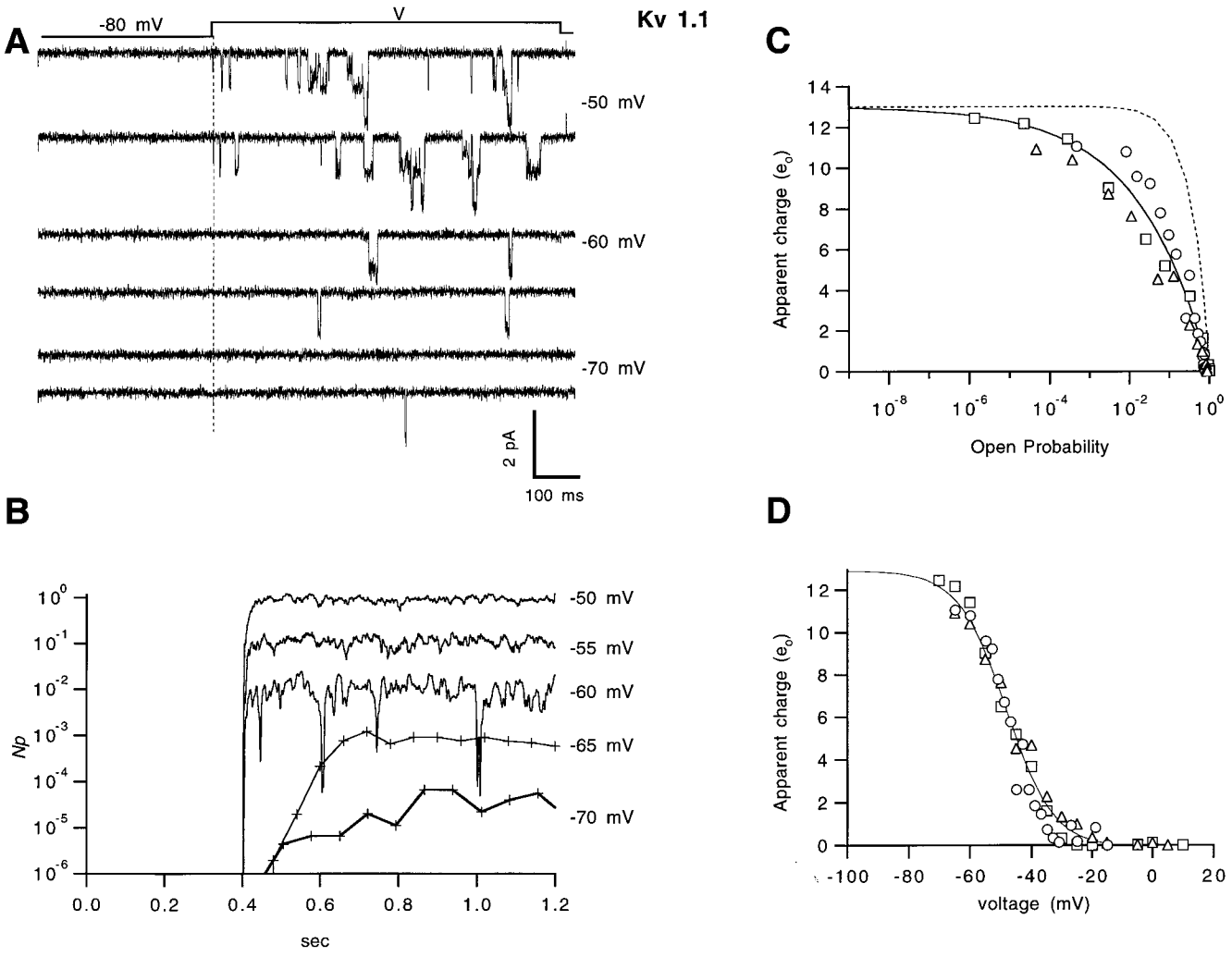

Figure 5. Limiting-slope measurement of the charge in Kv1.1 channels. (A) Single-channel openings from a cell-attached patch containing $n = 125$ channels, induced by 800-ms depolarizations from −80 mV to the potentials shown. (B) The reconstructed time course of *NP*, plotted semilogarithmically. (C) The apparent charge q_s, computed from *P*(V) according to Eq. 1 and plotted as a function of open probability *P*. The continuous curve is the fourth power of a Boltzmann function with a total charge of 13 e_o; the dotted curve is a single Boltzmann function with the same amount of charge. Different symbols represent different experiments. (D) Values of q_s as a function of voltage. The continuous curve is a fitted Boltzmann function representing the voltage dependence of charge movement, computed with q_T of 13 e_o.

The result of combining the single channel data with the values of N and P_{max} is shown in Fig. 6 C. The minimum measured value of the absolute open probability in this patch is $\sim 10^{-7}$ and the maximum, from noise analysis at 70 mV, was 0.71. At values of P between 10^{-7} and 10^{-4} exponential fits of the $P(V)$ relation yield an apparent charge q_s of 12.1 ± 0.5 e_o. A fourth power Boltzmann function with 12 or 13 e_o total charge (continuous curves) superimposes fairly well on the data (Fig. 6 C) when q_s is plotted as a function of *P*.

The same charge estimate results in comparing q_s with the macroscopic charge movement. The quantity superimposes well on the q_s data (Fig. 6 D) with the fitted value $q_T = 12.5$ e_o. Thus, this channel behaves as expected from Eq. 2 and the charge movement in the voltage range below that accessible to our q_s measurements is seen to be small. Our best estimate of the total charge for Kv2.1 is therefore 12.5 e_o.

It is unlikely that this estimate of total charge is in error due to inactivation or missed channel events. Inactivation in the Kv2.1 channels was measured with 500-ms prepulses (Fig. 7 A) and was found to be negligible at potentials below −50 mV (Fig. 7 B). Single-channel events at negative voltages show a single open-time component with a mean duration of 8 ms (Fig. 7 C), consistent with the presence of only one open state of the channel. The duration of bursts of openings, ~15 ms (Fig. 7 D), is essentially voltage independent, always

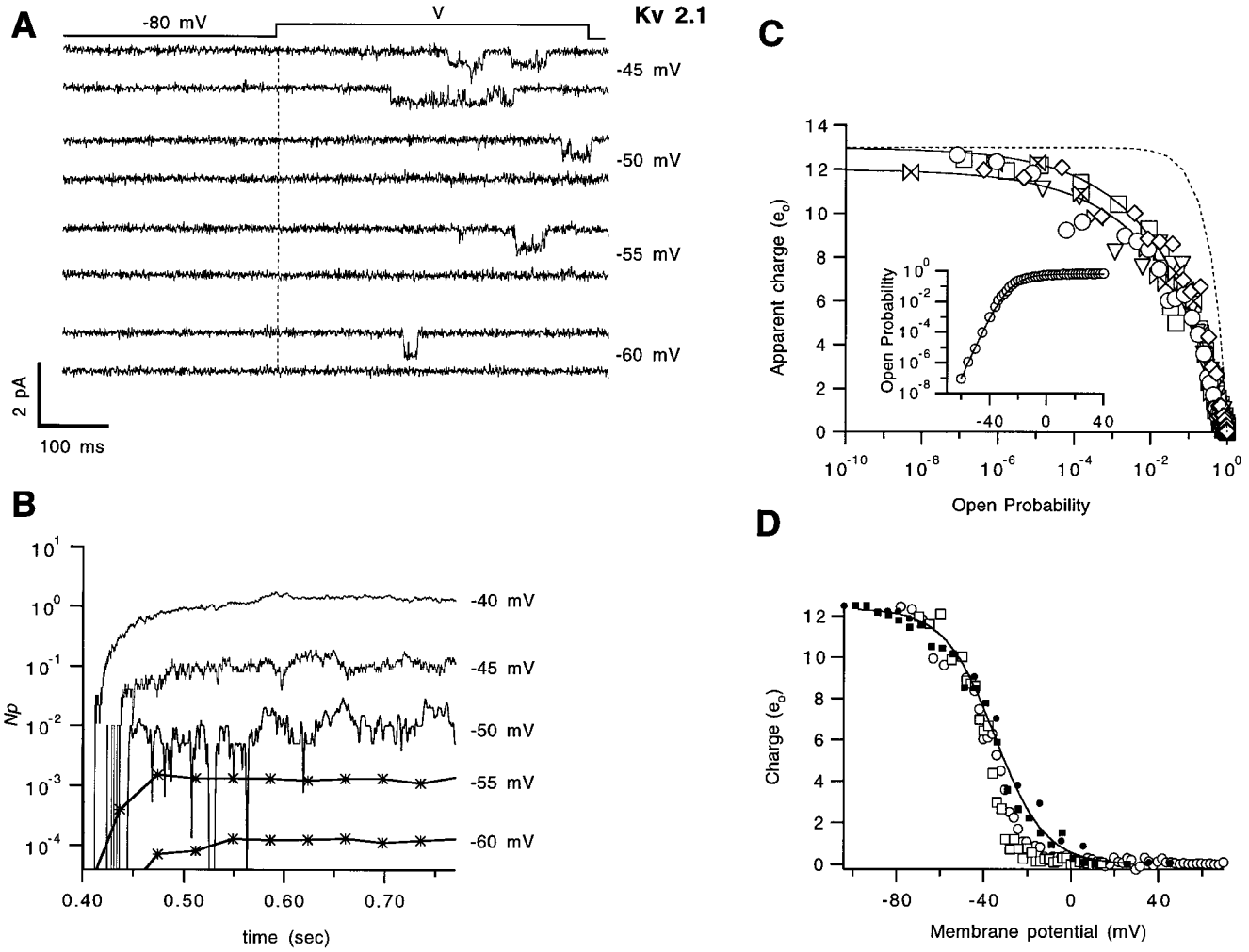

Figure 6. Limiting-slope measurement of the charge in Kv2.1 channels. (A) Single Kv2.1 channel events recorded at the indicated potentials after holding the patch for 400 ms at −80 mV. The data sweeps are not consecutive. Fluctuation analysis from macroscopic currents at 70 mV yielded an estimate of $N = 1{,}500$ channels. (B) Time course of *NP* obtained from the same patch in A; each trace represents the average of 300–400 idealized sweeps. (C) Open probabilities from six experiments transformed according to Eq. 1. Superimposed in the data are two solid curves showing the fourth power of a Boltzmann function scaled to a total charge of 12 and 13 e_o. The dotted curve is a simple Boltzmann function with 13 e_o. The inset depicts one experiment's voltage dependence showing the extent of the *P* values explored. (D) Voltage dependence of the apparent gating charge (open symbols), compared with $q_T\,[1 - \hat{Q}(V)]$, where $\hat{Q}(V)$ is the normalized charge movement derived from gating currents and q_T was 12.5 e_o (filled symbols). The continuous curve is a Boltzmann function calculated with a charge of 12.5 e_o.

much greater than the detection dead-time of 120 μs; thus, a very small and voltage-independent fraction of events is expected to be missed in the evaluation of *NP*.

Limiting-Slope Measurements in Shab Channels

In *Xenopus* oocytes, the expression of *Shab* channels was low, producing maximal whole-cell currents of ~10 μA at +40 mV. To obtain higher channel densities and to allow the possibility of whole-cell recording of *Shab* gating currents, we established a baculovirus expression system using Sf9 insect cells. The currents obtained in cell-attached patches from Sf9 cells infected with the *Shab* baculovirus have very similar characteristics to those recorded in patches in oocytes. No voltage-dependent currents were observed in whole-cell recordings from five uninfected Sf9 cells.

Subconductance levels. Interestingly, single *Shab* channels in single-channel patches and in recordings from multiple channel patches show a tendency to open to subconductance states. These events arise from *Shab* channels since direct transitions are observed between the subconductance and the fully open states. Fig. 8 A shows representative current recordings at −70 mV. Indicated are the fully open state and the substate level at 40% of the full open current level. It is evident that the

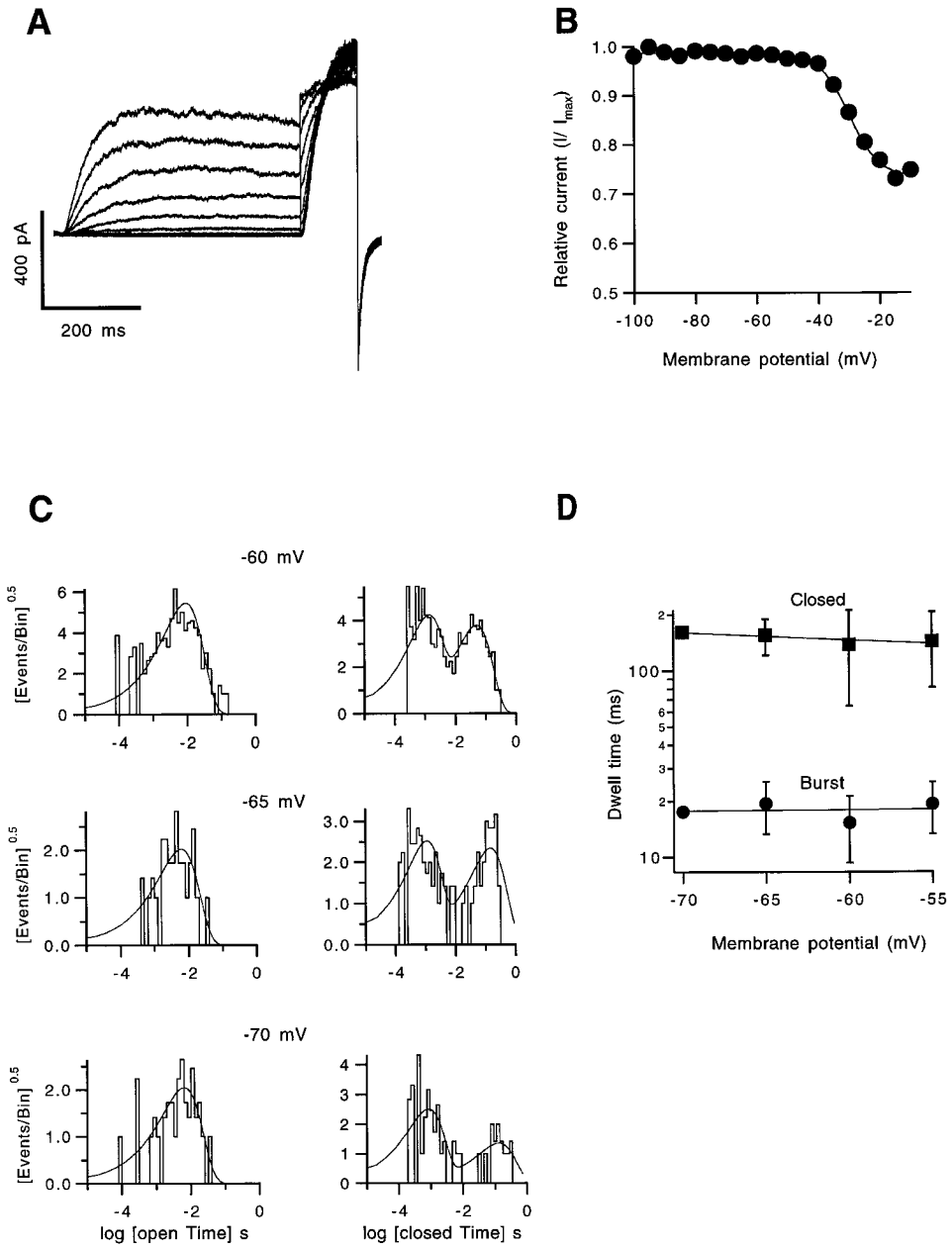

Figure 7. Ruling out artifacts in the estimation of charge in Kv2.1 channels. (A) Macroscopic Kv2.1 currents in response to a double-pulse protocol. The second pulse voltage was fixed at 20 mV and the potential of the 400-ms prepulse was varied from −100 to −10 mV. (B) Steady state inactivation function from the data in A. Plotted is the ratio of the current at the end of the second pulse to the current without prepulse, as a function of prepulse potential. The continuous curve is the function:

$$\frac{I}{I_0} = \frac{A}{1 + e^{-(V - V_0)q/kT}} + (1 - A),$$

where $A = 0.27$ is the maximum relative inactivation; $q = 5.2\ e_o$ and $V_o = -30$ mV. (C) Dwell-time distributions at negative voltages. Histograms in the left column are the open times and those in the right show the closed times. Superimposed are the maximum-likelihood fits to single and double exponential functions of the open and closed times, respectively. (D) Voltage dependence of the time constant of the long closed state and the mean burst duration. Plotted are mean values from four patches and the error bars show the standard deviation. The parameters of the fits (lines) are given in Table I.

channel can dwell only in the substate or make transitions to the open state with or without having to traverse the substate level.

Subconductance openings are more prominent at negative voltages. At −90 mV, less than one percent of the time is spent in the subconductance level, but 98% of the observed events are subconductance openings. This is illustrated in Fig. 8 B, where all-points histograms of current recordings from multichannel patches at the indicated potentials are shown. The intermediate Gaussian component fitted to the histogram corresponds to the substate and its integral is proportional to the probability of occupancy of the substate. At potentials more negative than −70 mV, the probability of the substate P_s is greater than the probability of the fully open state, *P*. These probabilities are plotted in Fig. 8 C; it is seen that while *P* increases monotonically, P_s increases and then decreases with depolarization. This characteristic of P_s, along with its smaller voltage dependence (the apparent charge is only 2.2 e_0 between −90 and −70 mV) is consistent with the sublevel representing an intermediate state in the activation pathway.

The voltage dependence of occupancies of the substate and the fully open state can be described by specific schemes. The steady state occupancy curves in Fig. 8 C were computed from the model shown in that figure in which sequential transitions bring the channel

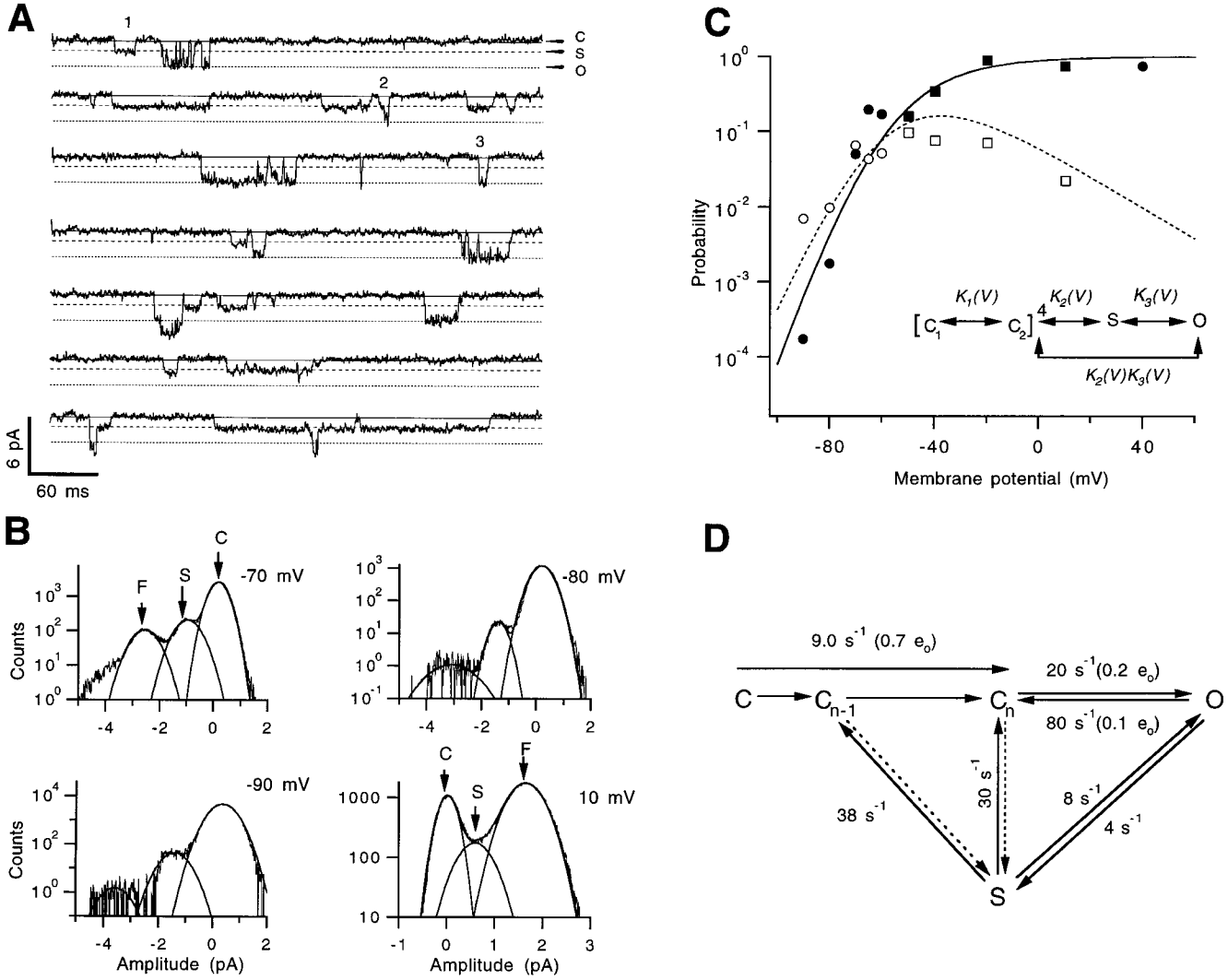

Figure 8. Substate kinetics in *Shab* channels. (A) Current traces at −70 mV from a patch containing three channels. The different horizontal dotted lines indicate the closed, substate, and full open levels. Note the various types of transitions indicated by the numbers. From the substate, a channel can either (1) close or (2) proceed to the fully open state; direct transitions from closed to fully open also occur (3). (B) All-point amplitude histograms from 200 sweeps at the indicated membrane potential. The histograms were fitted to a sum of three Gaussians and the individual components are shown. The letters identify the closed, substate, and fully open states according to the current amplitude. Absolute probabilities of being in the substate are: 0.078 at −70 mV, 0.012 at −80 mV, 0.0084 at −90 mV, and 0.021 at 10 mV. The probability of being in the fully open state are: 5.2×10^{-2} at −70 mV, 1.4×10^{-3} at −80 mV, 1.4×10^{-4} at −90 mV, and 0.75 at 10 mV. The histograms are from a patch containing three channels, except for the histogram at 10 mV, which is from a single-channel patch. (C) Steady state occupancies of the open (filled symbols) and subconductance (open symbols) states. Squares are data obtained from a one-channel patch in which the external K^+ concentration $[K^+]_o$ = 10 mM, and circles are from a multiple channel patch with $[K^+]_o$ = 60 mM. Points from the low $[K^+]_o$ patch have been shifted by −20 mV to approximately compensate for the shift in activation due to altered external potassium. The continuous curve represents the open-state probability as a function of voltage and the dotted curve is the probability of the substate, computed from the scheme shown, where the equilibrium constants at 0 mV and their effective charges are: K_1 = 1.18, 1.2 e_o; K_2 = 1.18, 0.6 e_o; K_3 = 2.4, 1.8 e_o. (D) Kinetic description of substate and opening transitions at negative potentials. Values of rate constants at −70 mV are given; in cases where a clear voltage dependence could be discerned over the voltage range of −90 to −65 mV, partial charges are also given in parentheses. The first latency to channel opening is roughly accounted for by the rate from state C to C_n (arrow at top left). Dotted arrows indicate transitions that occur but whose rates we could not determine.

to a substate (S), and then the fully open state. In the model, a parallel pathway also allows direct openings without passing through the substate; this provision is necessary because the substate is traversed in only ~6% of full openings of the channel. The model yields a limiting slope corresponding to a total charge of 7.2 e_o for the open state and 5 e_o for the substate.

Kinetic analysis of the substate was carried out to characterize the transitions near the open and subconductance states at negative potentials. The rate con-

stants for transitions away from the substate were obtained from the dwell-time distribution in the substate and the fraction of transitions occurring in each particular path. For example, at negative voltages, dwells in the substate were seen to be terminated by transitions to the open state, to a closed state, or transitions to a closed state followed, after a delay of ~50 ms, by channel opening. The rate constants k_{ij} were obtained:

$$k_{ij} = \frac{f_{ij}}{\tau_i},$$

where τ_i is the mean dwell time in state i and f_{ij} is the fraction of all transitions leaving state i that end in state j (Zheng and Sigworth, 1997). Dwell-time distributions in the fully open state were used to obtain rates for transitions to the closed state in the activation pathway identified as C_n, and to the substate, using the same method. Values of the rate constants for transitions near the open state obtained in this way are shown in Fig. 8 D, which is presented as an example of a scheme that can account for the kinetic phenomena we observe. In conclusion, both the steady state and kinetic behaviors are consistent with the subconductance level being associated with a state that is a kinetic intermediate and that is reached with less than the full charge movement.

Magnitude of charge movement. For the estimation of total charge movement, we ignore dwells at the sublevel because these reflect an intermediate state. Instead, we make use of only the probability *P* of the fully open state, which is the predominant state at large depolarizations. Sublevel dwells will not affect the estimation of *N* by noise analysis because they are brief and very rare at the test voltage of +60 mV.

Even ignoring the sublevels, activation of *Shab* channels is not as voltage dependent as that of Kv2.1. At a holding potential of −90 mV it is possible to observe channel openings, and *NP* for the fully open state is seen to change only 10-fold for 10-mV depolarizations (Fig. 9, A and B); this is about half the sensitivity seen for the other channel types. In constructing idealized traces, we took care not to confuse overlapping sublevel currents with open-state events; such overlapping events were very rare except at relatively depolarized voltages such as −70 mV. The resulting apparent charge estimate, based on *P* values between 10^{-5} and 10^{-3} was $q_l = 7.1 \pm 0.3$ e_o ($n = 2$; Fig. 9 C). Plotting q_s against *P*, the asymptotic value appears to be 7.5 e_o (Fig. 9 D). Similarly, low apparent charge values were seen in recordings from *Shab* channels in oocytes, where $q_l = 7.5 \pm 0.3$ e_o ($n = 3$) when evaluated over the range of *P* values from 10^{-6} to 10^{-4}. Whole-cell recordings of gating currents in Sf9 cells allow the comparison of macroscopic charge movements with the voltage dependence of q_s. The quantity superimposes fairly well on q_s values with $q_T = 7.5$ e_o (Fig. 9 E) and demonstrates that very little charge movement occurs at voltages negative to −90 mV. We therefore take 7.5 e_0 to be the estimate for the total charge in this channel.

Sigg and Bezanilla (1997) point out that limiting-slope estimates of charge can be in error when there are multiple open states of a channel. For example, our estimate for *Shab* charge could be in error if there were an additional open state O′, having indistinguishable conductance, connected to the main open state O through a voltage-dependent transition. For example, Scheme I could account for the "missing" 5 e_o of charge. To be consistent with the relatively shallow activation curve (Fig. 8 C), the transition from O to O′ would necessarily occur in the voltage range of −40 mV and above. This additional transition will give rise to a large gating-charge movement that occurs at depolarized potentials.

$$\underset{5e_o}{\overset{K_1}{C \leftrightarrow}} \underset{2.5e_o}{\overset{K_2}{S \leftrightarrow}} \underset{5e_o}{\overset{K_3}{O \leftrightarrow}} O' \qquad \text{(SCHEME I)}$$

A comparison of the voltage dependence of q_s with that predicted from $Q(V)$ indeed shows a small discrepancy of this sort: a minor component of the gating charge $Q(V)$ moves at potentials above −40 mV, where the q_s curve is essentially flat. This component is, however, much smaller than that expected from Scheme I and therefore is unlikely to arise from an additional open state. The discrepancy between q_s and $Q(V)$ is in fact similar to the discrepancies seen in *Shaker* and Kv2.1 channels (Figs. 4 E and 6 D). Because the discrepancy occurs in the voltage range of channel opening, we believe that it arises from an interaction of permeant ions with the open channel. Effects of permeating ions on activation gating have been studied in sodium channels (Townsend et al., 1997) and potassium channels (Swenson and Armstrong, 1981; Demo and Yellen, 1992; Chen et al., 1997) and effects on *Shaker* channels have been noted (Stefani et al., 1994; Schoppa and Sigworth, 1998a). In most cases, the presence of permeant ions is seen to result in the stabilization of the open state; meanwhile, blocking the ionic current with a toxin or pore mutation has an effect similar to the removal of extracellular ions.

We expect that, in the presence of permeant ions, the equilibrium of the final opening transition is shifted toward the open state, tending to increase the cooperativity of channel opening and resulting in a steeper voltage dependence of q_s. In our gating-current experiments, permeant ions were either absent or prevented from entering the pore, so the cooperative effect would be absent, yielding the shallower $Q(V)$ curves that are observed. We conclude that there is no evidence for a large, additional charge movement that occurs while the channel is open.

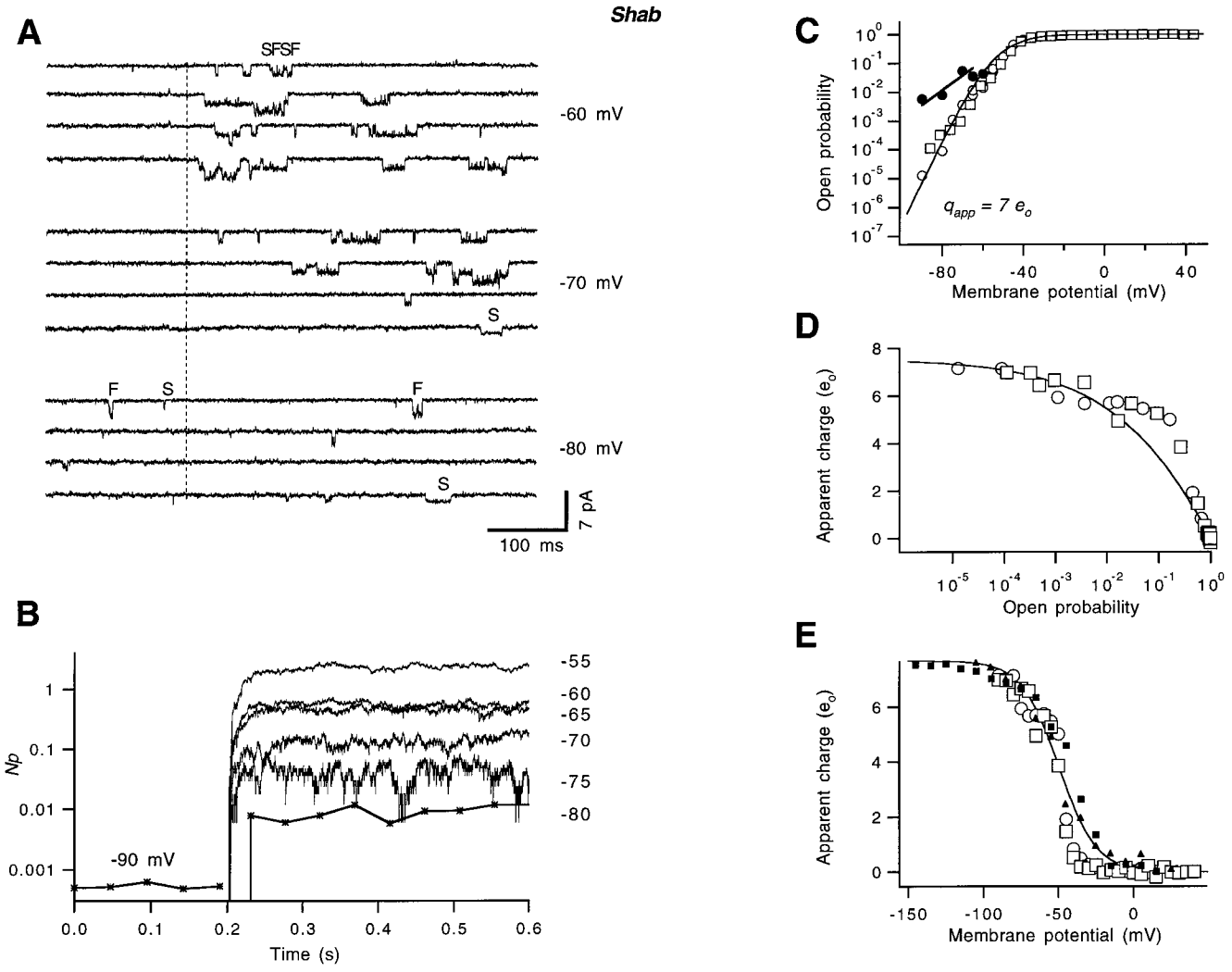

Figure 9. Limiting-slope measurements of *Shab* channels expressed in Sf9 cells. (A) Recordings of single channel openings at the indicated membrane potential in a cell-attached macro patch containing $N = 230$ channels, as estimated from noise analysis at 60 mV. The dotted line represents the start of the depolarization to the given voltage, from a holding potential of −90 mV. Some openings to the subconductance state are indicated as S and openings to the fully open conductance as F. (B) Time dependent (averaged) *NP* values obtained from the idealization of 300–400 traces such as those in A, in which only full openings were counted. (C) The complete activation curve for two patches obtained after combination of the single channel data with macroscopic [$G(V)$] data. The continuous curve is a fourth-power Boltzmann function with total gating charge of 7.5 e_o. (●) The occupancy of the subconductance state at negative voltages, fitted with an exponential function (solid line) with a charge of 2.2 e_o. (D) From the data in C, for the fully open state, the effective charge is plotted as a function of *P*. The continuous curve is the prediction from a fourth-power Boltzmann function with a charge of 7.5 e_o. (E) The same data plotted against voltage (open symbols). The filled symbols represent the function $q_T\,[1 - \hat{Q}(V)\,]$ derived from gating currents, with $q_T = 7.5$ e_o.

As a further check for the possible existence of multiple open states, we examined the single-channel kinetics of *Shab* channels. Fig. 10 A shows recordings from a patch containing a single *Shab* channel. Over the range of voltages from −30 to +40 mV, the open time distribution showed a single exponential component (Fig. 10 B). Data from multichannel patches also show no evidence for a second open-time component at voltages down to −80 mV. The mean burst duration at −60 mV is 3.7 ± 0.1 ms ($n = 3$) and has a very weak voltage dependence corresponding to a partial charge of 0.1 e_o. The single-exponential open-time distributions support the idea that *Shab* has only one fully open state. Thus again, we find no reason to expect multiple open states, and find the simplest conclusion to be that *Shab* channels have a reduced gating charge of ∼7.5 e_0.

Ideally, this estimate of gating charge should be confirmed with an independent measure in which the total integrated gating current is normalized by the number of channels. Unfortunately, the relatively low expression level of *Shab* channels has precluded this sort of measurement, which requires either the ability to measure gating currents in a patch membrane or the ability to measure radioligand binding to a single cell.

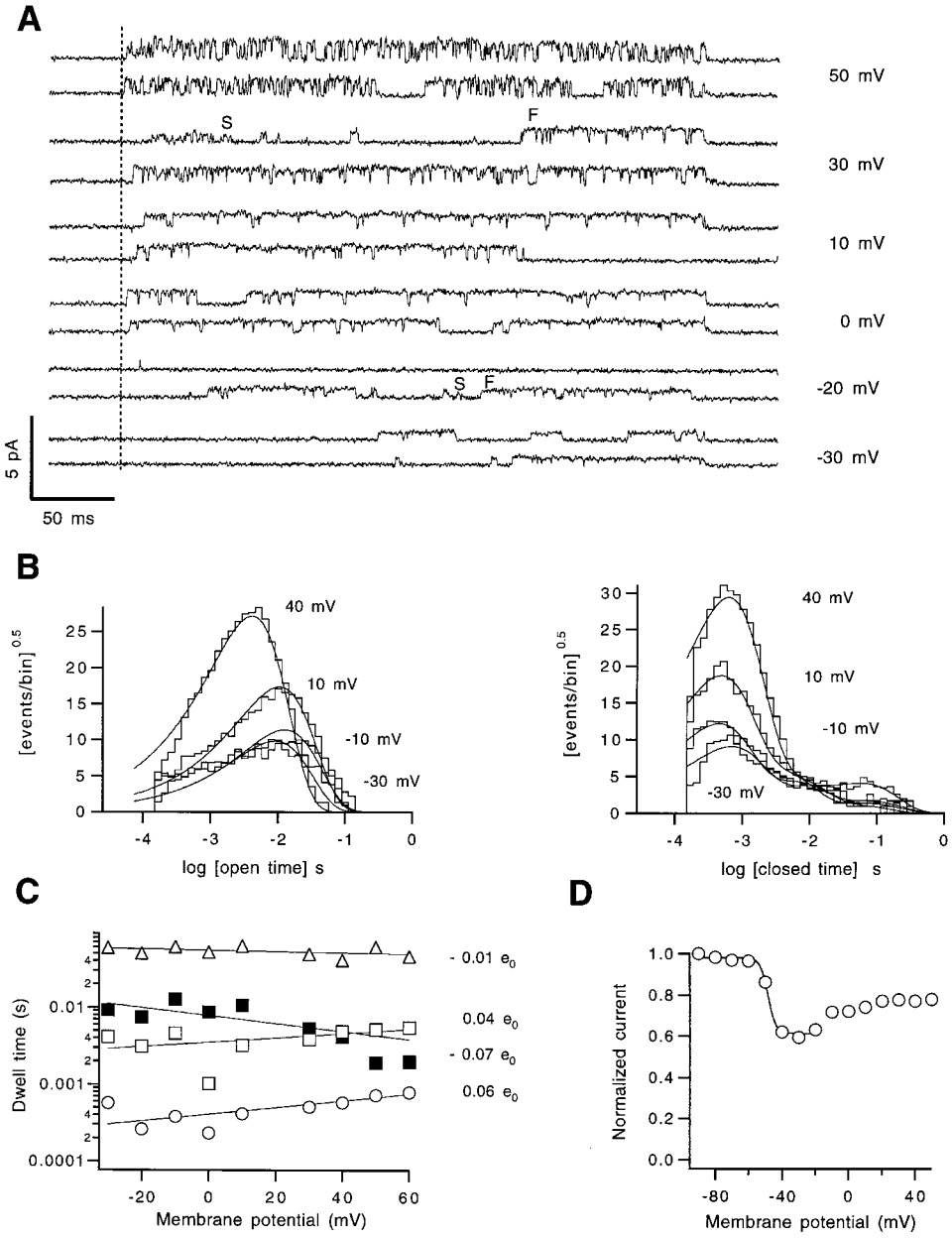

Figure 10. *Shab* channels appear to have only one fully open state. (A) Single-channel traces recorded from a cell-attached patch at the indicated voltages. The patch contained only one channel as judged from the absence of overlapping openings. S indicates subconductance events; F indicates full conductance events. Bath solution was the standard composition. The pipette contained (mM): 5 K-aspartate, 5 KCl, 1.8 $CaCl_2$, 100 NMDG-aspartate, 10 HEPES, pH 7.4. (B) Dwell-time distributions in the fully open (left) or closed (right) states. Superimposed on the histograms are maximum-likelihood fits to an exponential function for the open-time histogram, or a mixture of three exponentials for the closed time histogram. (C) Voltage dependence of the time constants. Filled symbols are the open-time constant and open symbols represent the three detected closed-time constants. The fitted lines represent exponential functions of voltage with the effective charges shown. (D) Prepulse inactivation in *Shab* channels. A prepulse of 500-ms duration was given at the indicated membrane potential and the current at a subsequent fixed depolarization of 40 mV was measured. The continuous curve is a fit to the same function as in Fig. 7 from −90 to −20 mV. The fit parameters are: $A = 0.39$, $q = 8.1\ e_o$, and $V_o = -47$ mV.

Single-channel kinetics. The *Shab* single-channel closed-time distributions were well described by three exponential components (Fig. 10 B). The fastest closures are most frequent at the largest depolarization of +40 mV. The dwell time in this closed state is essentially voltage independent (Fig. 10 C, △). This closed state may be the result of block by intracellular components or it could be a conformational state that is entered after the channel has opened, as is the case in *Shaker* channels (Hoshi et al., 1994). We favor the latter interpretation since the rapid closures are also observed in inside-out patch recordings where the only solutes bathing the internal membrane surface are K^+, aspartate, HEPES, and EGTA.

Transitions to this fast closed state from the open state accounts for the fact that P does not approach unity at large depolarizations. The value of P_{max} is 0.72, as obtained from noise analysis of macroscopic currents at +50 to +70 mV. From the single-channel recordings, we calculate an open probability of 0.68 at +60 mV, very close to the estimate from noise analysis.

Shab channels inactivate on a time scale of seconds and with a half-inactivation voltage of −30 mV (Tsunoda and Salkoff, 1995). To test for possible inactivation effects in our experiments, we measured the inactivation induced by 500-ms prepulses (Fig. 10 D). The reduction in current due to inactivation during depolar-

ization to −60 mV or below is seen to be at most 5%, which would have a negligible influence in our estimates of the voltage dependence of *P*.

DISCUSSION

In the experiments described in this report, we have estimated the effective gating charge of four members of the voltage-gated K^+ channel superfamily. We find that *Shaker* and Kv1.1 have an effective gating charge of ~13 e_o, as does the Kv2.1 channel. *Shab* channels, on the other hand, have an effective gating charge of only 7.5 e_o. The estimates of gating charge are based on measurements of the channel open probability *P* at negative membrane potentials where *P* is very small. The voltage dependence of *P* provides a lower-bound estimate on the total charge movement (Almers, 1978); in all channel types except Kv1.1, the reliability of the gating-charge estimate was confirmed by comparison of the voltage dependence of gating current according to the theory of Sigg and Bezanilla (1997). We have also determined that the probability of any voltage-independent openings is very small in these channels and that the charge movement is tightly coupled to channel opening in *Shaker* and Kv2.1.

In measuring the open probability, we are confronted with several possible sources of error. First, an artifactually large voltage dependence of *P* would result if the probability of missing brief channel openings increased substantially as the membrane potential was made more negative. We find, however, that the channel burst durations are weakly dependent on voltage in the range of potentials examined for each of the four channel types so that most bursts of openings are sufficiently long to be detected (Table I). The measurements in *Shaker* and *Shab* channels were the most susceptible to this effect, since the mean burst duration becomes <4 ms at −70 mV. This is nevertheless considerably longer than the minimum detectable event duration, 120 μs at our analysis bandwidth of 1.5 kHz, so that the error is negligible.

A second source of error would arise from voltage-dependent inactivation of channels, resulting in an artifactually reduced apparent voltage dependence. The known properties of *Shaker* channels, and tests for inactivation in Kv1.1, Kv2.1, and *Shab* channels, however, showed that inactivation effects were negligible under the conditions of our measurements.

Finally, our estimates of *P* to very low values make use of the assumption of a homogeneous population of channels; if a fraction of channels has a shifted voltage dependence, then the estimated voltage dependence of *P* would be distorted. Heterogeneity in the voltage dependence of single, mutant *Shaker* channels has been observed (Schoppa and Sigworth, 1998b), but this is of a form (a positive shift of a minority of the channels) that would have little influence on our estimates; such heterogeneity was not seen in the wild-type truncated *Shaker* channels studied here (Schoppa and Sigworth, 1998a). We encountered no evidence for such heterogeneity in the single-channel behavior of the other channel types; if it were present, it would reduce the apparent voltage dependence of *P* at intermediate voltages, but leave the asymptotic voltage dependence unaffected. We take the relatively good agreement between the voltage dependence of q_s and $\hat{Q}$ as evidence that errors from heterogeneity are small.

TABLE I

Voltage-dependent Characteristics of the Four Types of Channels Examined

Channel	P_{max} (+60)	P_{min}	q_s	t_{burst}	z_{burst}	q_T
			e_0	ms		e_0
Shaker	0.79 ± 0.02	10^{-7}	12.7 ± 0.3 (3)	4.0 ± 2.8 (3)	0.09	13
Kv1.1	0.84 ± 0.04	10^{-6}	11.5 ± 1.3 (3)	5.1 ± 0.1 (4)	0.06	13
Kv2.1	0.71 ± 0.04	10^{-7}	12.1 ± 0.5 (6)	15 ± 6 (3)	0.02	12.5
Shab	0.72 ± 0.03	10^{-5}	7.1 ± 0.3 (3)	3.7 ± 0.1 (2)	0.09	7.5

The quantity P_{max} is the estimated maximum open probability measured from nonstationary noise analysis at +60 mV; P_{min} is the minimum open probability used for the determination of the apparent charge q_s. The mean burst duration t_{burst} is given for a voltage of −60 mV, and the apparent valence z_{burst}, describing the reduction of burst duration with hyperpolarization, is also given. As described in the text, q_T is our best estimate for the total charge, obtained from extrapolation or curve fitting. Values are given as the mean ± SEM. Numbers in parentheses correspond to the number of experiments.

S4 Charges and Gating Charge Movements

Logothetis et al. (1993) observed that *Shab* channels have a low voltage sensitivity, only ~60% of that seen in Kv1.1 channels. They ascribed this difference to the differences in the S4 regions, where *Shab* has only five basic residues as compared with seven in the *Shaker* family channels. They also found a similar reduction in voltage sensitivity in Kv1.1 when the first (R1) and last (K7) basic residues were replaced with the neutral residues found in *Shab*, consistent with the idea that these two residues contribute to the gating charge in Kv1.1.

Our experiments, which provide limiting-slope estimates of charge to much lower open probabilities and which distinguish between the main conductance level and a subconductance state in *Shab*, nevertheless confirm the view that *Shab*'s total charge movement is much smaller, only 7.5 e_o, compared with 13 e_o in Kv1.1.

Other evidence from mutation studies is equivocal about the role of residues R1 and K7 in the voltage sensor. Early studies showed moderate effects on the voltage dependence of gating from the neutralization of these residues in *Shaker* (Papazian et al., 1991), but large effects from their neutralization in Kv1.1 (Liman et al., 1991; Logothetis et al., 1992). More rigorous

Shaker mutation studies involving the direct measurement of gating charge show a large decrease in charge when R1 is neutralized, but no effect from the neutralization of K7 (Aggarwal and MacKinnon, 1996; Seoh et al., 1996). Studies in which cysteines were placed at or near the R1 position of *Shaker* show that this residue undergoes a moderate, voltage-dependent change in accessibility to externally applied reagents PCMBS (Yusaf et al., 1996) and [2-(trimethylammonium)ethyl]methanethiosulfonate (MTSET; Larsson et al., 1996), leading Baker et al. (1998) to assign it an effective electrical distance change $\delta = 0.5$. Meanwhile, near K7, no voltage-dependent accessibility change is seen (Larsson et al., 1996). From these studies, one concludes that, in *Shaker*, R1 seems to contribute to the gating charge movement, while K7 does not.

In view of these results, the large charge movement in Kv2.1 channels, indistinguishable from that in *Shaker* channels, comes as a surprise. Like *Shab*, Kv2.1 has only five basic residues in S4, and serves as a counterexample to the requirement of R1 for full charge movement. Instead, this result is consistent with the idea originally proposed by Larsson et al. (1996) that only the central five S4 residues participate in the gating charge movement.

Previous estimates of the gating charge of Kv2.1 are much smaller than ours, in the range of 4–6 e_o. They were obtained from the steepness of channel activation over the range of open probabilities from 0.005 to 0.1 (Taglialatela and Stefani, 1993) or from the fit of macroscopic and other kinetic data to a particular sequential gating scheme (Benndorf et al., 1994). The relatively small charge values can be understood from the limited range of *P* values that were measured by these authors; only at negative potentials where *P* is smaller than $\sim 10^{-5}$ is an asymptotic steepness corresponding to 13 e_o approached (Fig. 6 C). It should be kept in mind that our experiments made use of a channel with mutations in the outer pore region, but it seems to us very unlikely that these mutations could underlie an increased voltage sensitivity of the channels.

Why is the behavior of *Shab* so different from its mammalian homologue Kv2.1? In these channels, the sequences of S2, S3, and S4 are very well conserved, with identical charged residues. Since the gating charge movement arises from charges within the protein (Sigworth, 1994), it seems inescapable that it is the degree of movement of charged groups in the membrane field, rather than the total charge, that is reduced in *Shab* compared with Kv2.1. It is not difficult to imagine how the degree of movement could be decreased. Charge movement in voltage-gated channels occurs in multiple steps; in *Shaker* channels, at least two, and probably three or more, sequential, charge-moving conformational changes occur in each subunit (Zagotta et al., 1994; Bezanilla et al., 1994; Schoppa and Sigworth, 1998c). Perhaps in *Shab* channels one of these steps does not occur, limiting the total charge movement to $\sim$60% of that of *Shaker*.

Strict Coupling of Charge Movement to Channel Opening

Ligand-gated ion channels show a finite open probability even in the absence of agonists. The mouse muscle acetylcholine receptor channel has a spontaneous open probability of $\sim 5 \times 10^{-6}$ (Jackson, 1988), while cyclic nucleotide–gated channels have spontaneous open probabilities on the order of 10^{-5} to 10^{-3} (Ruiz and Karpen, 1997; Tibbs et al., 1997). The activation of these channels is well described by allosteric models in which the open state is stabilized by the binding of ligands. In the present study, we find that the voltage-insensitive open probability of *Shaker* channels is very much smaller, $<10^{-9}$; this suggests an obligatory coupling of charge movement to channel opening rather than a traditional allosteric mechanism. At the most negative potentials studied here, the steepness of the open probability curve does not decrease, and the effective charge computed from that steepness agrees well with other estimates of the total gating charge per channel. Taken together, these results imply that essentially all of the charge movement is obligatorily coupled to channel opening; that is, *Shaker* channels cannot open unless all of the charge movement has occurred in each subunit. The only exception to this obligatory coupling is a small, weakly voltage-dependent charge movement in *Shaker* channels that has been recently described by Stefani and Bezanilla (1996).

The same strict coupling between charge movement and channel opening is seen in Kv2.1 channels, where we have estimated the voltage-insensitive open probability to be $<4 \times 10^{-8}$, and in sodium channels, where the open probability has been measured down to 10^{-7} (Hirschberg et al., 1995). The situation is, however, different in *Shab* channels, where even at -90 mV the probability of occurrence of a subconductance state was the relatively large value of 8×10^{-3}. This subconductance state appears to represent an intermediate step in channel activation, becoming predominant only at negative potentials. Subconductance states representing kinetic intermediates in channel activation have been observed in Kv2.1 and *Shaker* channels (Chapman et al. 1997; Zheng and Sigworth, 1998), but isolated openings to these levels were not detected in our measurements because either their lifetimes were too short or their equilibrium occupancies were even lower than that of the main conductance state, under the conditions we used.

As might be expected for the reduced voltage sensitivity requirement of delayed-rectifier potassium channels, *Shab* channels have a much lower voltage depen-

dence of channel activation. They also have less gating charge movement than the A-type *Shaker* channel and its homologue, Kv1.1, which also produces transient currents when coexpressed with beta subunits (Rettig et al., 1994). It is surprising that the homologous mammalian delayed rectifier Kv2.1 does not have a similarly reduced charge movement. It will be interesting to see what is the molecular origin of this difference.

We thank Dr. R. MacKinnon for providing the Kv2.1 construct and Agitoxin, and Dr. D. Logothetis (Mount Sinai Medical Center, New York, NY) for Kv1.1 and *Shab* DNA. We also thank Y.-Y. Yan for expert technical assistance and Y. Yang, J. Zheng, Q.-X. Jiang, T. Rosenbaum, and S. Basavappa for helpful comments.

This work was supported by National Institute of Health grant NS 21501.

Submitted: 18 May 1999 Revised: 17 September 1999 Accepted: 20 September 1999 Released online: 25 October 1999

REFERENCES

Aggarwal, S., and R. MacKinnon. 1996. Contribution of the S4 segment to gating charge in the *Shaker* K^+ channel. *Neuron*. 16:1169–1177.

Almers, W. 1978. Gating currents and charge movements in excitable membranes. *Rev. Physiol. Biochem. Pharmacol.* 82:96–214.

Baker, O.S., H.P. Larsson, L.M. Mannuzzu, and E.Y. Isacoff. 1998. Three transmembrane conformations and sequence-dependent displacement of the S4 domain in *Shaker* K^+ channel gating. *Neuron*. 20:1283–1294.

Benndorf, K., R. Koopmann, C. Lorra, and O. Pongs. 1994. Gating and conductance properties of a human delayed rectifier K^+ channel expressed in frog oocytes. *J. Physiol.* 477:1–14.

Bezanilla, F., E. Perozo, and E. Stefani. 1994. Gating of *Shaker* K^+ channels. II. The components of gating currents and a model for channel activation. *Biophys. J.* 66:1011–1021.

Chandy, K.G., and G.A. Gutman. 1995. Voltage-gated potassium channel genes. *In* Ligand and Voltage-gated Channels. Handbook of Receptors and Channels. R.A. North, editor, CRC Press LLC., Boca Raton, FL. 1–71.

Chapman, M.L., H.M.A. Van Dongen, and A.M.J. Van Dongen. 1997. Activation-dependent subconductance levels in the drk1 K^+ channel suggest a subunit basis for ion permeation and gating. *Biophys. J.* 72:708–719.

Chen, F.S.P., D. Steele, and D. Fedida. 1997. Allosteric effects of permeating cations on gating currents during K^+ channel deactivation. *J. Gen. Physiol.* 110:87–100.

Colquhoun, D., and F.J. Sigworth. 1995. Fitting and statistical analysis of single-channels records. *In* Single Channel Recording. B. Sakmann and E. Neher, editors. Plenum Publishing Corp., New York, NY. 483–587.

Connor, J.A., and C.F. Stevens. 1971a. Voltage clamp studies of a transient outward membrane current in gastropod neural somata. *J. Physiol.* 213:21–30.

Connor, J.A., and C.F. Stevens. 1971b. Prediction of repetitive firing behavior from voltage clamp data on an isolated neuron soma. *J. Physiol.* 213:31–53.

Demo, S.D., and G. Yellen. 1992. Ion effects on gating of the Ca^{++}-activated K^+ channel correlate with occupancy of the pore. *Biophys. J.* 61:639–648.

Frech, G.C., A.M. VanDongen, G. Schuster, A.M. Brown, and R.H. Joho. 1989. A novel potassium channel with delayed rectifier properties isolated from rat brain by expression cloning. *Nature.* 340:642–645.

Gross, A., T. Abramson, and R. MacKinnon. 1994. Transfer of the scorpion toxin receptor to an insensitive potassium channel. *Neuron*. 13:961–966.

Heinemann, S.H., and F. Conti. 1992. Nonstationary noise analysis and application to patch clamp recording. *In* Methods in Enzymology. B. Rudy and L. Iverson, editors. Academic Press, Inc., San Diego, CA. 131–148.

Hirschberg, B., A. Rovner, M. Lieberman, and J. Patlak. 1995. Transfer of twelve charges is needed to open skeletal muscle Na^+ channels. *J. Gen. Physiol.* 106:1053–1068.

Hodgkin, A.L. 1975. The optimum density of sodium channels in an unmyelinated nerve. *Philos. Trans. R. Soc. Lond. B Biol. Sci.* 270: 297–300.

Hoshi, T., W.N. Zagotta, and R.W. Aldrich. 1994. *Shaker* potassium channel gating. I. Transitions near the open state. *J. Gen. Physiol.* 103:249–278.

Jackson, M.B. 1988. Dependence of acetylcholine receptor channel kinetics on agonist concentration on cultured mouse muscle fibers. *J. Physiol.* 397:555–583.

Koren, G., E.R. Liman, D.E. Logothetis, B. Nadal-Ginard, and P. Hess. 1990. Gating mechanism of a cloned potassium channel expressed in frog oocytes and mammalian cells. *Neuron*. 2:39–51.

Larsson, H.P., O.S. Baker, D.S. Dhillon, and E.Y. Isacoff. 1996. Transmembrane movement of *Shaker* K^+ channel S4. *Neuron*. 16: 387–397.

Liman, E.R., P. Hess, F. Weaver, and G. Koren. 1991. Voltage-sensing residues in the S4 region of a mammalian K^+ channel. *Nature*. 353:752–756.

Logothetis, D.E., B.F. Kammen, K. Lindpaintner, D. Bisbas, and B. Nadal-Ginard. 1993. Gating charge differences between two voltage-gated K^+ channels are due to the specific charge content of their respective S4 regions. *Neuron*. 10:1121–1129.

Logothetis, D.E., S. Movahedi, C. Satler, K. Lindpaintner, and B. Nadal-Ginard. 1992. Incremental reductions of positive charge within the S4 region of a voltage-gated K^+ channel result in corresponding decreases in gating charge. *Neuron*. 8:531–540.

Lopatin, A.N., and C.G. Nichols. 1994. Internal Na^+ and Mg^{2+} blockade of DRK1 (Kv2.1) potassium channels expressed in *Xenopus* oocytes. *J. Gen. Physiol.* 103:203–216.

Lopez-Barneo, J., T. Hoshi, S.H. Heinemann, and R.W. Aldrich. 1993. Effects of external cations and mutations in the pore region on C-type inactivation of *Shaker* potassium channels. *Receptors Channels*. 1:61–71.

Neher, E. 1971. Two fast transient current components during voltage clamp on snail neurons. *J. Gen. Physiol.* 58:36–53.

Noceti, F., P. Baldelli, X. Wei, N. Qin, L. Toro, L. Birnbaumer, and E. Stefani. 1996. Effective gating charges per channel in voltage-dependent K^+ and Ca^{2+} channels. *J. Gen. Physiol.* 108:143–155.

Papazian, D.M., L.C. Timpe, Y. Jan, and L.Y. Jan. 1991. Alteration of voltage-dependence of *Shaker* potassium channel by mutations in the S4 sequence. *Nature.* 349:305–310.

Perozo, E., R. MacKinnon, F. Bezanilla, and E. Stefani. 1993. Gating currents from a nonconducting mutant reveal open–closed conformations in *Shaker* K^+ channels. *Neuron*. 11:353–358.

Rettig, J., S.H. Heinemann, F. Wunder, C. Lorra, D.N. Parcej, J.O.

Dolly, and O. Pongs. 1994. Inactivation properties of voltage-gated K^+ channels altered by presence of beta-subunit. *Nature*. 369:289–294.

Ruiz, M.L., and J.W. Karpen. 1997. Single cyclic nucleotide–gated channels locked in different ligand-bound states. *Nature*. 389: 389–392.

Schoppa, N.E., K. McCormack, M. Tanouye, and F.J. Sigworth. 1992. The size of gating charge in wild-type and mutant *Shaker* potassium channels. *Science*. 255:1712–1715.

Schoppa, N.E., and F.J. Sigworth. 1998a. Activation of *Shaker* potassium channels. I. Characterization of voltage-dependent transitions. *J. Gen. Physiol*. 111:271–294.

Schoppa, N.E., and F.J. Sigworth. 1998b. Activation of *Shaker* potassium channels. II. Kinetics of the V2 mutant channel. *J. Gen. Physiol*. 111:295–311.

Schoppa, N.E., and F.J. Sigworth. 1998c. Activation of *Shaker* potassium channels. III. An activation gating model for wild-type and V2 mutant channels. *J. Gen. Physiol*. 111:313–342.

Schwarz, T.L., D.M. Papazian, R.C. Caretto, Y.N. Jan, and L.Y. Jan. 1988. Multiple potassium channel components are produced by alternative splicing at the *Shaker* locus in *Drosophila*. *Nature*. 331: 137–142.

Seoh, S.A., D. Sigg, D.M. Papazian, and F. Bezanilla. 1996. Voltage sensing residues in the S2 and S4 segments of the *Shaker* K^+ channel. *Neuron*. 16:1159–1167.

Sigg, D., and F. Bezanilla. 1997. Total charge movement per channel. The relation between gating charge displacement and the voltage sensitivity of activation. *J. Gen. Physiol*. 109:27–39.

Sigworth, F.J. 1980. The variance of sodium current fluctuations at the node of Ranvier. *J. Physiol*. 307:97–129.

Sigworth, F.J. 1994. Voltage-gating of ion channels. *Q. Rev. Biophys*. 27:1–40.

Sigworth, F.J., and S.M. Sine. 1987. Data transformations for improved display and fitting of single-channel dwell time histograms. *Biophys. J.* 52:1047–1054.

Smith-Maxwell, C.J., J.L. Ledwell, and R.W. Aldrich. 1998. Uncharged amino acids and cooperativity in voltage-dependent potassium channel activation. *J. Gen. Physiol*. 111:421–439.

Stefani, E., and F. Bezanilla. 1996. Voltage-dependence of the early events in voltage-gating. *Biophys. J.* 70:A131. (Abstr.)

Stefani, E., L. Toro, E. Perozo, and F. Bezanilla. 1994. Gating of *Shaker* K^+ channels. I. Ionic and gating currents. *Biophys. J.* 66: 996–1010.

Stühmer, W., F. Conti, H. Suzuki, X.D. Wang, M. Noda, N. Yahagi, H. Kubo, and S. Numa. 1989. Structural parts involved in activation and inactivation of the sodium channel. *Nature*. 339:597–603.

Swenson, R.P., and C.M. Armstrong. 1981. K^+ channels close more slowly in the presence of external K^+ and Rb^+. *Nature*. 291:427–429.

Taglialatela, M., and E. Stefani. 1993. Gating currents of the cloned delayed-rectifier K^+ channel DRK1. *Proc. Natl. Acad. Sci. USA*. 90: 4758–4762.

Tibbs, G.R., E.H. Goulding, and S.A. Siegelbaum. 1997. Allosteric activation and tuning of ligand efficacy in cyclic-nucleotide gated channels. *Nature*. 386:612–615.

Townsend, C., H.A. Hartmann, and R. Horn. 1997. Anomalous effect of permeant ion concentration on peak open probability of cardiac Na^+ channels. *J. Gen. Physiol*. 110:11–21.

Tsunoda, S., and L. Salkoff. 1995. Genetic analysis of *Drosophila* neurons: *ShalShaw* and *Shab* encode most embryonic potassium currents. *J. Neurosci*. 15:1741–1754.

Yang, Y., Y. Yan, and F.J. Sigworth. 1996. How does the W434F mutation block current in *Shaker* potassium channels? *J. Gen. Physiol*. 109:779–789.

Yusaf, S.P., D. Wray, and A. Sivaprasadarao. 1996. Measurement of the movement of the S4 segment during activation of a voltage-gated potassium channel. *Pflügers Arch*. 433:91–97.

Zagotta, W.N., T. Hoshi, J. Dittman, and R.W. Aldrich. 1994. *Shaker* potassium channel gating. II. Transitions in the activation pathway. *J. Gen. Physiol*. 103:279–319.

Zheng, J., and F.J. Sigworth. 1998. Selectivity changes during activation of mutant *Shaker* potassium channels. *J. Gen. Physiol*. 110: 101–117.